GEOMETRICAL ANALYSIS AND OPTIMIZATION OF 5-AXIS MILLING PROCESSES

by

Lütfi Taner TUNÇ

Submitted to the Graduate School of Engineering and Natural Sciences

in partial fulfillment of

the requirements for the degree of Master of Science

in

SABANCI UNIVERSITY

Spring 2006

GEOMETRICAL ANALYSIS AND OPTIMIZATION OF 5-AXIS MILLING
PROCESSES

APPROVED BY:

Assoc. Prof. Dr. Erhan BUDAK ……………….

(Dissertation Supervisor)

Assist. Prof. Dr. Selim BALCISOY ………………………

Assist. Prof. Dr. Güllü KIZILTAŞ …………………….

Assist. Prof. Dr. Bülent ÇATAY …………………….

Assist. Prof. Dr. Tonguç ÜNLÜYURT …………………….

DATE OF APPROVAL: ………………………

GEOMETRICAL ANALYSIS AND OPTIMIZATION OF 5-AXIS MILLING
PROCESSES

Lütfi Taner TUNÇ

Industrial Engineering, MSc Thesis, 2006

Thesis Supervisor: Assoc. Prof. Dr. Erhan BUDAK

Keywords: CL-File, 5-Axis milling, Sculptured surface machining, Machining strategy, 5-Axis milling geometry, Process optimization, Process simulation, Selection of machining parameters.

Abstract

5-axis milling processes are widely used in industries where complex surfaces are machined, and cutter accessibility is limited due to geometrical constraints on the workpiece. Additional motion capability increases the accessibility of the cutting tool, so it becomes possible to machine complex surfaces despite the geometrical constraints. In most of these industries dimensional tolerance integrity, surface quality, and productivity are of great importance. Therefore, identification of optimal or near-optimal process conditions, and selection of appropriate machining strategy for a given workpiece are required. Increased motion capability in 5-axis complicates the geometry and the mechanics of the process. Thus, optimization of 5-axis milling processes becomes a complex engineering problem. In order to solve such a problem, process models should be used together with geometrical analysis methods. In selection of appropriate machining strategy, surface characteristics should be known together with the process mechanics. In this thesis, a complete geometrical model is presented for 5-axis milling processes using ball-end mills. The developed model is integrated with an existing 5-axis process model in order to simulate the cutting forces throughout a given toolpath. Also, the effect of lead and tilt angle pair on process mechanics is investigated, and optimized values of those under various conditions are identified. In addition, a model suggesting the most appropriate strategy among various machining strategies for roughing and finishing operations for regular free form surfaces is presented. The developed models are verified through experiments and their applications are demonstrated on complex surfaces.

5-EKSEN FREZELEME SURECLERININ GEOMETRİK ANALİZİ VE OPTİMİZASYONU

Lütfi Taner TUNÇ

Endüstri Mühendisliği, Yüksek Lisans Tezi, 2006

Tez Danışmanı: Doç. Dr. Erhan BUDAK

Özet

5 eksen frezeleme süreçleri karmaşık yüzeylerin ve parça üzerinde geometrik kısıtların olduğu, havacılık, kalıp ve otomotiv endüstrilerinde yaygın olarak kullanılmaktadır. Yüksek hareket kabiliyeti, kesici takımın parçaya ulaşmasını kolaylaştırdığından, geometrik kısıtlara rağmen karmaşık yüzeylerin üretilmesi mümkün hale gelmektedir. Bu tür endüstrilerde boyutsal tolerans bütünlüğü, yüzey kalitesi ve üretim verimliliği çok önemlidir. Bu yüzden, en iyi ya da en iyiye yakın süreç koşullarının belirlenmesi ve en uygun kesme stratejisinin seçilmesi gereklidir. 5-eksen frezeleme süreçlerindeki yüksek hareket kabiliyeti süreç geometrisini ve mekaniğini karmaşıklaştırır. Bunun sonucu olarak, 5-eksen frezeleme süreçlerinin eniyilemesi karmaşık bir mühendislik problemi haline dönüşür. Bu problemi çözmek için süreç modelleri, geometrik çözümleme yöntemleriyle birlikte kullanılmalıdır. Kesme stratejisi seçiminde ise yüzey karakteristiği ve süreç mekaniği dikkate alınmalıdır. Bu tezde, küresel uçlu takım kullanan 5-eksen frezeleme süreçleri için tam bir geometrik çözümleme modeli sunulmuştur ve 5-eksen süreç modeliyle birlikte kullanılıp süreç benzetimi yapılmıştır. Süreç mekaniğine etkisi olan takım açılarının değişik koşullar için en iyi değerleri araştırılmıştır. Ayrıca, kesme stratejilerini çeşitli kriterlere göre karşılaştırıp en uygun stratejiyi bir model geliştirilmiştir. Geliştirilen modeller deneysel olarak doğrulanmış ve karmaşık yüzeyler üzerindeki uygulamaları gösterilmiştir.

ACKNOWLEDGEMENTS

TABLE OF CONTENTS

LIST OF FIGURES

LIST OF TABLES

Chapter 1

Introduction

Machining is one of the widely used manufacturing processes in industry. The main idea is removing the desired amount of material volume in form of small chips by means of a cutting tool. There are various types of machining operations such as turning, broaching, milling, drilling etc. Milling operations are applied where high level of manufacturing flexibility is needed. Therefore it is an important operation for machining industry. One of the most widely used milling operations is 5-axis milling which is an important process for aerospace, die-mold and automotive industries. It is widely used in manufacturing of mechanical parts having free form, complex surfaces such as turbine blades, dies-molds and aircraft structural parts. (See Figure 1-1) 5-axis milling operations are performed using the machine tools shown in Figure 1-2. These machine tools may be configured in various types; six of them are given in Figure 1-3 [8]. Since kinematics and dynamics of each configuration is different, each of them may be used for particular industries or parts.

Figure 1-1: Products machined using 5-axis milling.

There are several challenges in such industries. One of the most important challenges is achieving high part quality. This leads high manufacturing tolerances and dimensional tolerance integrity. Another challenge is increasing the productivity. In order to increase the productivity the optimized values of machining parameters and appropriate machining strategies should be identified for a given workpiece geometry. Those can be identified using process models together with the geometrical models developed for 5-axis milling processes.

Figure 1-2: 5-axis machine tool
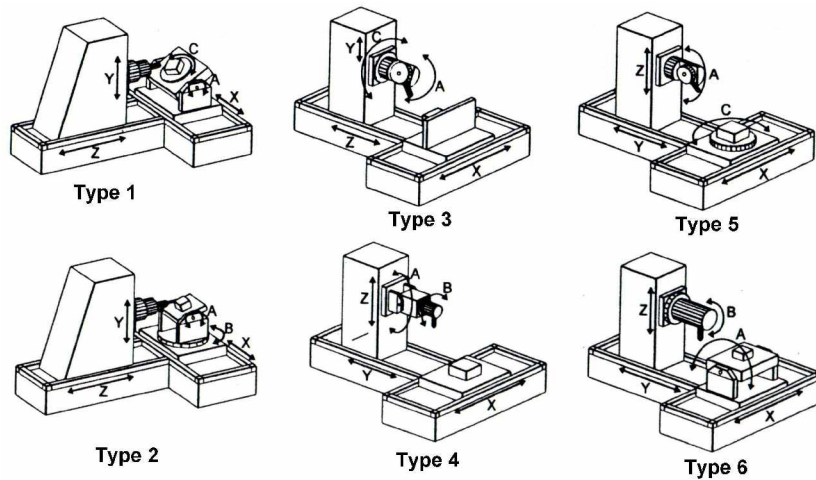
Figure 1-3: Possible configurations of 5-axis machine tools

Geometry of 5-axis milling processes depends on several geometrical parameters which are mainly related to tool geometry and workpiece geometry. Geometrical parameters are namely depths of cut and lead-tilt angles. Interaction between the cutter and workpiece is illustrated in Figure 1-4. Since there is a complex interaction between workpiece and tool having insight into the process beforehand is beneficial to identify improved process conditions. For such a purpose, a process simulation should be performed. In the simulation, process information is parsed from a Cutter Location (CL) file where only the orientation and the center position of the tool are given. The geometrical parameters required in the process simulations are not

explicitly given in the CL-file. Thus, it is required to extract those through geometrical analysis.

Figure 1-4: Workpiece – cutter interaction in 5-axis milling

In 5-axis milling processes, various machining strategies can be applied. Selection of the most appropriate machining strategy for a given workpiece is of great importance from the productivity and the part quality points of view. In strategy selection, both the surface characteristic and process mechanics play important roles. Thus, it is required to develop a model which evaluates different strategies from process mechanics and surface geometry points of view. In addition, it would be beneficial to investigate whether a new strategy can be proposed for a given workpiece. In most of the industrial applications, process parameters and machining strategies are decided based on experience or trial and error methods. Therefore, models developed in this thesis would be significantly useful for industrial applications.

1.1   Research Objective

The main objective of this research is to develop methods and strategies for modeling, analysis and optimization of 5-axis milling processes. In order to achieve and implement this objective, the necessary steps can be summarized as follows:

i.   Extract geometrical parameters from a given CL-file and workpiece geometry for 5-axis milling operations.

ii.   Simulate cutting forces throughout a given process using the extracted geometrical information and the available process models.

iii.   Determine the optimum tool orientation and other machining parameters using simulations.

iv.   Develop a method for evaluation and optimal selection of common machining strategies available in CAD/CAM systems

v.   Integrate the geometry and process models for analysis, simulation and optimization of 5-axis milling operations.

1.2   Organization of the Thesis

The thesis is organized as follows: Review of related literature is presented in this chapter, followed by the geometry of ball-end mill and 5-axis milling geometry in Chapter 2 where the required geometrical values related to the ball-end are calculated. Depths of cut and lead-tilt angles are defined in a coordinate system which consists of feed, crossfeed and surface normal vectors where surface normal vector is obtained using a reference CL-file. Calculation methodology of the named geometrical parameters is presented in Chapter 3. Depths of cut are calculated using the workpiece geometry information together with the tool position and orientation where, lead-tilt angles are calculated by applying matrix transformations. These are followed by verification of the methods on different workpiece geometries and process simulation methodology for a given toolpath and workpiece geometry in Chapter 4 where, experimental verification is also provided. Process optimization is presented in Chapter 5. Optimum values for lead & tilt angles under various conditions are investigated and

results are verified by experiments. Besides tool orientation, methodology developed for optimization of other machining parameters such as depths of cut and feed rate is presented. Machining strategy evaluation and selection methodology is also performed. Methodology to evaluate various machining strategies from process mechanics and surface characteristics points of view is given. In Chapter 6, applications of developed methods are presented Thesis is concluded with the summary of contributions and future work in Chapter 7.

1.3 Literature Review

The importance of process simulation has increased as a result of increased need for productivity and quality in machining operations. However, process simulation requires powerful geometrical and mechanics models. In literature, significant amount of work is available in milling geometry modeling. 3-axis and 5-axis ball-end milling of sculptured surface geometries are modeled using various methods. In addition, some literature is also available in optimization and machining strategy selection. However, only a very few of these studies consider a truly 5-axis process including the effects of tool orientation. Also, the machining strategies are evaluated with respect to either process mechanics or workpiece geometry. In this chapter an overview of the published works are given.

1.4 Process Geometry

Milling process geometry can be modeled using both analytical and discrete methods. Discrete methods are applicable to very complex geometries. However, they are slower with respect to the analytical methods. As in other problems, there is a compromise between the calculation time and the accuracy. Recent developments in CAD techniques enable analytical methods to be applied although they are applicable to limited complexity.

One of the noted discrete methods is vector clipping which is proposed by Chappel [5]. In this method, the part surface is approximated with cloud of points. Then, the surface normal vectors are calculated at various points. In order to simulate the machining process, the intersection of each vector with the tool swept envelope should be calculated. Another discrete method is the CSG which was first applied by Voelcker [31]. In this method, workpiece geometry is updated using Boolean operations.

In the Z-mapping method, the corresponding height of each grid point is stored as a Z-value. For each movement of the tool, Z-values are compared with the tool position and Z-values are updated. Anderson [1] proposed Z-mapping in collision detection and elimination in NC machining. Kim et al. [15] used Z-mapping technique to determine cutter contact area in 3-axis sculptured surface ball end milling. In Lazoglu's study [18] Z-mapping is used to determine the chip load. Kyu et al. [20] developed an enhanced Z-mapping method, by applying the super sampling technique. Thus the efficiency and accuracy of the Z-mapping method is increased. One of the applications of this method in 5-axis milling is the one presented by Fussel et al. [12]. In this study, tool-workpiece engagement was identified using an extended Z-buffer method. They used swept envelope of the cutter, to determine the intersection between the tool and Z-buffer elements. Also, the 5-axis movement of the tool was approximated as a 3-axis motion by keeping a desired accuracy.

Voxel and Octree are 3-D solid discrete methods. Voxel has a simple database, so its application is easy and fast. Also, workpiece stock update can be performed fast. Walstra et al. [32] applied this method to simulate the material removal from the stock in milling operations. Kim et al. [16] used Octree method to identify cutting regions in milling operations.

In analytical methods information of the workpiece geometry is used together with the tool position to analyze and simulate the process geometry. Book of Choi [7] presents a detailed theory and application of surface modeling techniques for CAD/CAM of complex surface geometries. One of the analytical studies in 3-axis sculptured surface machining is the one presented by Meng et al., [23]. Another book of Choi, et al. [8] presents a detailed theory and applications of 5-axis sculptured surface machining. Du et al., [10] and Bailey et al., [2] developed analytical methods to simulate 5-axis tool motion and process geometry. Ozturk et al., [25] analytically modeled the chip load in ball-end milling of free form surfaces. Lee et al., [19]

estimated the depth of cuts by positioning the tool axis coincident with the surface normal at that point. Imania et al., [14] modeled the cutter-workpiece engagement boundaries using a geometric simulation system which uses a commercial solid modeler ACIS© [34] as the geometric engine.

In this thesis, a practical and powerful method for integration of process models with machining geometry is proposed. In the proposed method, CL file is used as the main information source. The ball-end of the tool is modeled as a sphere. Tool position and orientation is used with the analytical information of the workpiece to perform geometrical analysis. Information of the machined surface is obtained from a reference CL file.

1.5 Process Optimization & Machining Strategy Evaluation

In production, process time and part quality vary conversely. Thus, optimization methods should be used to compromise between them. By use of optimization methods, cutting strategy and cutting conditions can be selected.

Optimization of process parameters such as the feed rate is one of the obvious objectives of such studies. One of the noted works in feed rate scheduling for 3-axis ball-end milling is presented by Lim, et al. [21]. In this study, the surface is divided into grid points. At each grid point the maximum feed rate direction is determined. Therefore, both cutting direction and feed rate optimization are performed. In another study which is presented by Erdim, et al. [11], feedrate scheduling is performed for 3-axis ball-end milling, based on both MRR and cutting forces. One of the first attempts for feed rate scheduling in 5-axis milling is presented by Bailey, et al. [3] as seen from the current studies, by applying feed rate scheduling techniques, cutting forces can be kept under a desired level. In addition, machining time of a given process can be decreased. In this respect such techniques are useful to improve 3 and 5-axis machining processes.

Another challenge in 5-axis milling is the selection of the tool orientation. For the optimization of the tool orientation, there are mainly two approaches. A common one is based on the kinematics smoothing of the tool axis movement. Another approach is to evaluate the tool orientation by considering the process mechanics. Ming, et al. [24] studied the former method, i.e. the tool orientation smoothing. They tried to

prevent abrupt changes in the tool orientation by applying quaternion interpolation algorithm. One of the studies which consider the effects of process mechanics on resulting surface is presented by Lim, et al. [22]. In this study, various tool orientations for a 5-axis turbine blade machining case are evaluated totally experimentally. This study provides some idea on the effect of tool orientation on the resulting surface quality. Though, the outcomes of this study can not be generalized over all workpiece and tool combinations since the study is not based on any modeling approach. In this respect, such a technique may be beneficial for only investigations on particular workpiece and tool pair. However, optimization of tool orientation is not enough by itself other machining parameters such as depths of cut, feed rate etc. should be optimized to minimize the overall machining time. This is not a straightforward task since there are several limitations such as tool breakage, deformation, chatter vibrations, available spindle torque and power. In the literature, Tekeli, et al. [30] developed a model which maximizes chatter-free material removal rate in end milling operations. In this study, optimal radial and axial depths of cut pairs are identified to minimize the overall machining time for a 3-axis pocketing operation.

Machining strategy evaluation and optimization are performed using both experimental and analytical methods in the literature. One drawback of experimental method is that; they are applicable to only workpiece and tool pairs used in the experiments. One of the experimental approaches is presented by Ramos et al. [27] where the effects of machining strategies on complex surface machining are analyzed. . Three different strategies namely, radial, raster and 3D offset, are compared from surface quality and texture aspects. Baptista et al. [4] analyzed the effects of machining parameters on surface roughness in 3 and 5-axis machining of complex surfaces experimentally. Two of the analytical approaches in strategy optimization are carried out by Giri, et al. [13] and Chu, et al.[9]. In both of the studies only the surface characteristics are considered for selection of the appropriate machining strategy. For finishing operations, consideration of surface characteristics is beneficial to improve resulting surface quality and decrease machining time. In a recent study, Lopez, et al. [17] determined local machining directions in finishing operations with respect to deformation of the cutter. So, by choosing the direction which leads to minimum tool deformation, overall surface error is reduced. For roughing operations, it is required to investigate the effects of process mechanics since relatively high material removal rates are approached and cutter is subjected to relatively high cutting forces.

In this thesis, a methodology to optimize cutter orientation under various machining conditions i.e. depths of cut, is proposed. The main idea is investigating the effect of tool orientation on the process mechanics by performing simulations. For this purpose, under different depths of cut values, process simulations are performed in a range of lead and tilt angles. In addition, a model which determines optimum or near optimum machining parameters to minimize machining time is proposed by considering the previously mentioned limitations. Various machining strategies are evaluated and compared considering both process mechanics and surface characteristics for roughing and finishing operations respectively. For each strategy, machining time is estimated and taken into account in comparison. In addition, optimal cutting directions are determined. Also, the determined directions are partitioned in order to find possible sub-regions where single machining pattern can be applied. By doing so, the surface can be divided into various sub-regions and different patterns can be applied on the surface if preferable.

1.6   Summary

In this chapter, an overview of studies on modeling of process geometry and mechanics for 3-axis and 5-axis milling of sculptured surfaces is given. Also, studies on machining parameter optimization and machining strategy evaluation are summarized. In the literature both analytical and discrete methods are used in 5-axis milling geometry modeling. Tool orientations are evaluated totally experimentally any process modeling approach is not applied. Studies which consider process mechanics in cutter path optimization and evaluation for roughing operations are limited to 3-axis ball end milling.

Chapter 2

Geometry of Ball-End Mill & 5-Axis Milling

2.1   Introduction

Due to increased contouring capability, ball-end mills are widely used in 5-axis milling operations. Thus, the geometry of 5-axis milling processes and ball-end mill tools are closely related. In this chapter, ball-end mill tool geometry and geometry of 5-axis milling processes are presented.

Figure 2-1: Ball-end mill

2.2 Geometry of Ball-End Mill

The detailed geometry of a ball-end mill tool is given in Figure 2-2. There are several parameters which defined ball-end mill geometry. Though, the ones used in this thesis are defined in this section. A Cartesian coordinate system is defined at the tool tip point, O. Local radius, Ra, of the ball-end at any axial location, z is defined as follows:

$$Ra(z)=\sqrt{R^2-(R-z)^2} \tag{2.1}$$
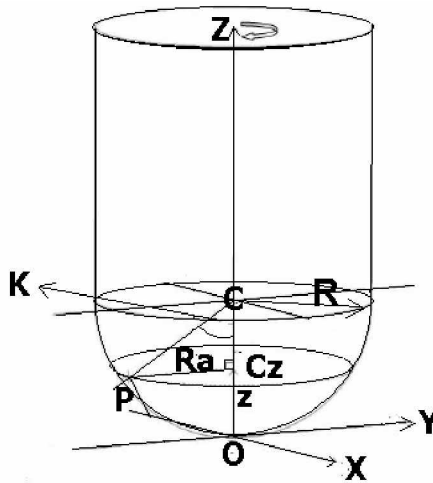
Figure 2-2: Ball-end mill geometry

2.3 5-Axis Milling Geometry

From the process geometry point of view, as the tool immerses into the workpiece, flutes on the tool start engaging with the workpiece material and generating chips. Thus, the engagement boundaries are of great importance for cutting force calculations. Tool-workpiece engagement boundaries are defined by four geometrical parameters which are namely the axial and radial depths of cut and the lead-tilt angles. Since these four parameters define the engagement boundaries, they should be determined based on the available information. . In addition, the coordinate systems where the process and the geometry are defined should also be formulated. In this section, coordinate systems used in calculations and geometrical parameters are defined.
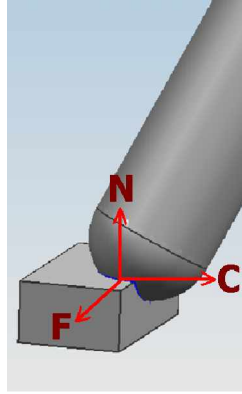
Figure 2-3: Tool immersion.

2.3.1   Coordinate Systems

Coordinate systems namely, workpiece coordinate system (WCS) and process dependent coordinate system (FCN) are used in geometrical calculations. World Coordinate System, WCS, consists of X, Y and Z where FCN is established by feed (F), crossfeed (C) and surface normal (N). WCS and FCN are illustrated in Figure 2-4. Since F, C, N vectors establish an orthogonal basis, coordinate transformation procedures given in [8] are valid for FCN. In the CL file, the data is given in WCS coordinates. On the other hand, geometrical parameters are defined in FCN coordinates. Thus, the relation between these two coordinate systems should be established consistently.
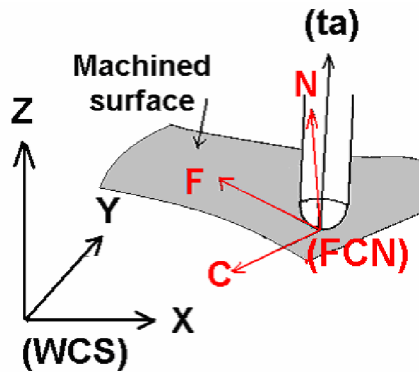
Figure 2-4: Coordinate systems

2.3.2   Definition of Lead and Tilt Angles

In 5-axis milling, the additional motions of the cutter are the two rotary axes. Cutter orientation is defined by lead and tilt angles which are measured between the tool axis and the surface normal. Lead angle is the rotation of the tool about the crossfeed vector (C), where tilt angle is about the feed vector (F) with respect to machined surface normal. Lead and tilt angles are shown in Figure 2-5. The lead and tilt angles are defined in FCN.

(a) Lead Angle   (b) Tilt Angle
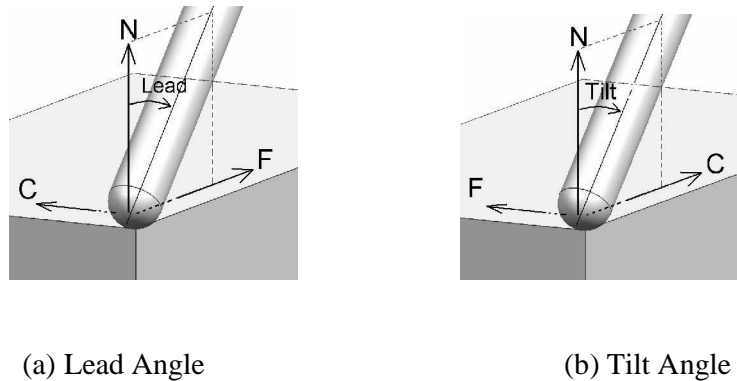
Figure 2-5: Lead and Tilt Angles

2.3.3   Definition of Depths of Cut

Besides the lead and tilt angles, the other required geometrical parameters are the depth of cuts. From the process geometry aspect, as the tool immerses into the workpiece, the flutes on the cutter start to engage with the workpiece. Force model calculates the cutting forces using the engagement boundaries between each flute and workpiece. These boundaries are identified by the depth of cuts, lead and tilt angles, and the tool geometry. Depths of cut are the axial (a) and radial (r) immersions of the tool into the workpiece, which are shown in Figure 2-6.
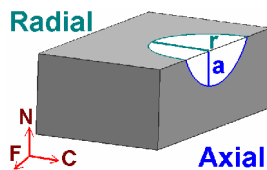
Figure 2-6: Depth of cuts, (r) and (a).

2.4   Summary

In this chapter, ball-end mill geometry and 5-axis milling geometry are presented. The coordinate systems used in geometrical analysis and geometrical parameters are defined. Two coordinate systems are used in calculations, namely FCN and WCS. The information parsed from the CL file is in WCS coordinates, where the geometrical parameters are defined in FCN. Lead angle is the rotation angle of the tool axis around cross feed direction with respect to surface normal. Tilt angle is rotation about feed direction. Depths of cut are defined with respect to radial and axial immersions of the tool into the workpiece.

Chapter 3

Calculation of Geometrical Parameters

3.1   Introduction

Geometrical parameters, namely depth of cuts and lead-tilt angles are required by the force and deformation models for process simulation. Moreover, even when it is not intended to perform a process simulation, it is convenient to have the information on those parameters, in order have a foresight into a given 5-axis milling process. Geometrical parameters are calculated by gathering the information on the tool position, process dependent vectors and workpiece geometry. In calculation of those geometrical parameters 2 coordinate systems are used and several coordinate transformations are performed between those. Tool position and process information are obtained from a CL file where, the information on the geometrical parameters is not given explicitly. Therefore, the CL file can not be used directly in the simulations but can be used together with the workpiece geometry information to extract the required parameters. Calculation procedure of geometrical parameters is illustrated in Figure 3-1.
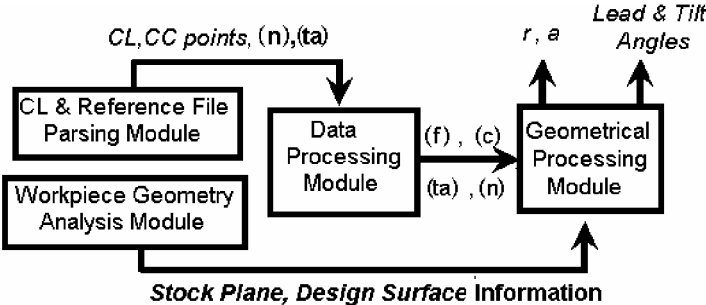
Figure 3-1: Geometrical calculation procedure

3.2   Processing of CL-File

In this thesis, CL file is used as the main geometric information source. In order to use the tool position and orientation in the geometrical calculations a separate module is created to parse the data from the CL file. In this section, the methodology for parsing the data is presented. The limitations of the developed methodology are discussed, and suggestions for improvement are given.

3.2.1   Parsing the Tool Position and Orientation

In general, CL file contains several motion commands such as "GO TO", "CIRCLE" and "RAPID". However, in 5-axis machining of sculptured surfaces, tool traverses point to point on the surface. This is performed by "GO TO" and "RAPID" commands when the cutter is in cut and out of cut respectively. (See Figure 3-2) The CL file also provides the tool tip coordinates and unit tool axis vector following the motion command.

```
TOOL PATH/FIN,TOOL,D8R4
TLDATA/MILL,8.0000,4.0000,75.0000,0.0000,0.0000
PAINT/PATH
PAINT/SPEED,10
LOAD/TOOL,0
SELECT/TOOL,0
PAINT/COLOR,31
FEDRAT/MMPM,250.0000
RAPID/-0.8324,0.2024,-5.0000,0.000000,0.000000,1.000000
GOTO/-0.8324,0.2024,-4.2964,-0.0081374,-0.0511923,0.9986557
GOTO/-0.6574,0.2024,-4.2582,-0.0088368,-0.0511923,0.9986497
GOTO/-0.4724,0.2024,-4.2170,-0.0086080,-0.0511923,0.9986517
GOTO/-0.2802,0.2024,-4.1730,-0.0068430,-0.0511923,0.9986654
              X       Y      Z          i          j          k

PAINT/COLOR,36
RAPID/27.5163,0.2024,-4.0411,0.3401654,-0.0511923,0.9389712
RAPID/27.7057,0.2024,-4.0645,0.3442156,-0.0511923,0.9374940
PAINT/COLOR,31
GOTO/-0.8322,0.5990,-4.2964,-0.0081861,-0.0513947,0.9986449
```

Figure 3-2: Portion of a CL File

3.2.2 Distinguishing Cutting Steps and Passes

In almost all of the generated CL files, there are several cutting steps. Cutting step is illustrated as the black lines in Figure 3-4. However, this information is not explicitly provided in the CL file. This is tackled in the following manner. CL files include the color index for in cut, air cut and step over etc. portions of a tool path. For each type of motion unique color index is provided by the "PAINT" command as shown in Figure 3-2. By tracking the color index following each "PAINT" command, start and end of each cutting step is identified.
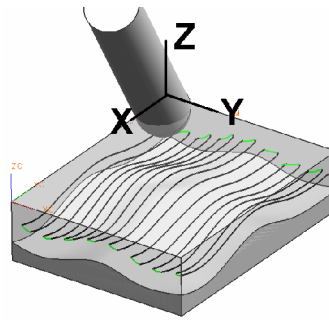
Figure 3-3: Illustration of cutting step.

In most of the applications, the CL files for roughing, semi-finishing and finishing passes are generated separately. However they may be in the same CL file in some cases. If there are multiple passes on the same surface stock, at the start of each cutting step, the tool position and the orientation are compared with the values of the 1st point of the 1st cutting step. If compared values are within the pre-defined tolerances this is considered as the start of a new pass. Besides the tool position and the orientation, feed rate, spindle speed and tool geometry are also available in the CL file. Information on those parameters is also parsed for further use in the geometrical calculations and process simulations.

3.3 Establishing FCN Coordinate System

As mentioned before, tool position and process information are obtained from a CL file where, data is given in WCS. On the other hand, lead and tilt angles are defined

in FCN. Therefore, FCN should be established and the values in the CL file should be transformed into FCN in order to attain uniformity in coordinate systems. In this manner calculating feed, cross feed and surface normal vectors accurately is vital. In 5-axis milling, coordinates of the tool tip, i.e. the CL point, is available in the CL file. Since tool has a continuously changing spatial motion, cutter contact point, i.e. the CC point, differs from CL point as shown in Figure 3-4. Due to this difference, it is required to calculate (f) between consecutive CC points. Besides, calculation of CC point requires (n) vector. This creates a recursive relation between (n) and (f) as shown in Figure 3-5. This recursive relation could be solved by using iterative methods. Since iterative methods compromise between time and calculation accuracy, instead of using iterative methods, this situation is tackled in the following manner. A reference file is generated where lead and tilt angles are chosen to be zero and all other process parameters being same with the original file. So, in the reference file, CL and CC points are obtained same, besides tool axis (ta) is coincident with (n). The benefit of this method is obtaining CC points and (n) without loss of accuracy. Finally, (f) and (c) are calculated as follows:

$$(\mathbf{f}) = \frac{\left[(x_{n+1}\text{-}x_n);(y_{n+1}\text{-}y_n);(z_{n+1}\text{-}z_n) \right]}{\text{norm} \left| P_n\ P_{n+1} \right|} \tag{3.1}$$

$$(\mathbf{c}) = (\mathbf{n}) \times (\mathbf{f}) \tag{3.2}$$

where, $P_n=(x_n,\ y_n,\ z_n)$, is the nth CC point and $P_{n+1}=(x_{n+1},\ y_{n+1},\ z_{n+1})$ is the $(n+1)^{st}$ CC point. By calculating unit (f) (c) and (n) vectors, FCN is established. Any vector, (u) given in WCS is transformed into FCN as follows:

$$\begin{bmatrix} u_f \\ u_c \\ u_n \end{bmatrix}_{(FCN)} = \begin{bmatrix} f_X\ f_Y\ f_Z \\ c_X\ c_Y\ c_Z \\ n_X\ n_Y\ n_Z \end{bmatrix} \begin{bmatrix} u_X \\ u_Y \\ u_Z \end{bmatrix}_{(WCS)} \tag{3.3}$$

Where, $(\mathbf{i}) = \begin{bmatrix} i_X \\ i_Y \\ i_Z \end{bmatrix}_{(WCS)}$ and $(\mathbf{i}) = (\mathbf{f}), (\mathbf{c}), (\mathbf{n})$.
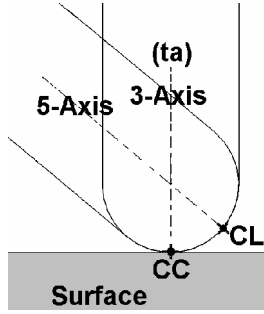
Figure 3-4: CC and CL points.
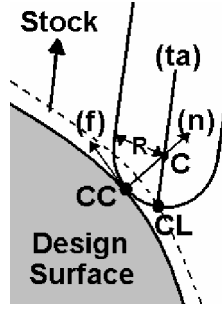
Figure 3-5: CC, CL and (n) relation.

3.4 Calculating Tool Axis by Given Lead & Tilt Angles

The major difference between 3-axis and 5-axis milling is the existence of lead and tilt angles. As mentioned previously, two of the required geometrical parameters are those. Before investigating the lead-tilt calculation method, it is convenient to analyze the calculation of tool axis (ta) by given lead and tilt angles for completeness. Tool axis is coincident with surface normal when those are both zero. So, it is considered that, the surface normal is rotated by the lead and tilt about crossfeed and feed vectors respectively. The rotation is concatenation of two basic rotations, where first by lead, then by tilt. In WCS, rotation about any unit vector (u) is performed using the following transformation matrix [5].

$$R(u,\theta) = \begin{bmatrix} u_x^2 + (1-u_x^2)C & u_x u_y V + u_z S & u_x u_z V - u_y S \\ u_x u_y V - u_z S & u_y^2 + (1-u_y^2)C & u_y u_z V + u_x S \\ u_x u_z V + u_y S & u_y u_z V - u_x S & u_z^2 + (1-u_z^2)C \end{bmatrix} \tag{3.4}$$

If u = i or j, rotation matrix given in (3.4) reduces to the following form [5] :

20

$$R(i,\theta) = \begin{bmatrix} 1 & 0 & 0 \\ 0 & C & S \\ 0 & S & C \end{bmatrix} R(j,\theta) = \begin{bmatrix} C & 0 & -S \\ 0 & 1 & 0 \\ S & 0 & C \end{bmatrix}$$

<div align="right">(3.5)</div>

Where, $C = \cos\theta$, $S = \sin\theta$, $V = vers\theta = (1-\cos\theta)$, $(\mathbf{u}) = \begin{bmatrix} u_X \\ u_Y \\ u_Z \end{bmatrix}$.

Since FCN is an orthogonal basis, rotation matrices given in (3.5) are valid when (u)=(f) or (c). Finally, the rotation is performed as follows.

$$\begin{bmatrix} C_{tilt} & 0 & S_{tilt} \\ 0 & 1 & 0 \\ -S_{tilt} & 0 & C_{tilt} \end{bmatrix} \begin{bmatrix} 1 & 0 & 0 \\ 0 & C_{lead} & -S_{lead} \\ 0 & -S_{lead} & C_{lead} \end{bmatrix} \mathsf{x} \begin{bmatrix} 0 \\ 0 \\ 1 \end{bmatrix}_{(FCN)} = (\mathbf{ta}) = \begin{bmatrix} ta_f \\ ta_c \\ ta_n \end{bmatrix}_{(FCN)}$$

<div align="right">(3.6)</div>

The rotation transformation matrix T, is given as below

$$T = \begin{bmatrix} C_{lead} & 0 & S_{lead} \\ S_{tilt}S_{lead} & C_{tilt} & -S_{tilt}C_{lead} \\ -C_{tilt}S_{lead} & S_{tilt} & S_{tilt}C_{lead} \end{bmatrix}$$

<div align="right">(3.7)</div>

3.5 Calculating Lead & Tilt Angles by Given Tool Axis

Problem of lead-tilt calculation resembles an inverse kinematics problem. Once FCN is established, the tool axis (ta) vector in WCS is obtained from CL file; lead-tilt angles are calculated in the following manner. First, the tool axis vector is transformed into FCN as follows.

$$\begin{bmatrix} ta_f \\ ta_c \\ ta_n \end{bmatrix}_{(FCN)} = \begin{bmatrix} f_X & f_Y & f_Z \\ c_X & c_Y & c_Z \\ n_X & n_Y & n_Z \end{bmatrix} \begin{bmatrix} ta_X \\ ta_Y \\ ta_Z \end{bmatrix}_{(WCS)}$$

<div align="right">(3.8)</div>

Then, equating (3.6) and (3.8) the following equation is obtained.

$$\begin{bmatrix} f_X\ f_Y\ f_Z \\ c_X\ c_Y\ c_Z \\ n_X\ n_Y\ n_Z \end{bmatrix} \begin{bmatrix} ta_X \\ ta_Y \\ ta_Z \end{bmatrix}_{(WCS)} = \begin{bmatrix} C_{lead} & 0 & S_{lead} \\ S_{tilt}S_{lead} & C_{tilt} & -S_{tilt}C_{lead} \\ -C_{tilt}S_{lead} & S_{tilt} & S_{tilt}C_{lead} \end{bmatrix} \begin{bmatrix} 0 \\ 0 \\ 1 \end{bmatrix}_{(FCN)} \tag{3.9}$$

$$\begin{bmatrix} f_X\ f_Y\ f_Z \\ c_X\ c_Y\ c_Z \\ n_X\ n_Y\ n_Z \end{bmatrix} \begin{bmatrix} ta_X \\ ta_Y \\ ta_Z \end{bmatrix}_{(WCS)} = \begin{bmatrix} S_{lead} \\ -S_{tilt}C_{lead} \\ S_{tilt}C_{lead} \end{bmatrix}_{(FCN)} \tag{3.10}$$

Finally, the lead and tilt angles are extracted by solving (3.10) as follows.

$$\begin{aligned} lead &= \arctan2(a, \sqrt{b^2 + c^2}) \\ tilt &= \arctan2\left(-b, c\right) \end{aligned} \tag{3.11}$$

where, $a = \mathrm{dot}\left[(\mathbf{ta}),(\mathbf{f})\right]$, $b = \mathrm{dot}\left[(\mathbf{ta}),(\mathbf{c})\right]$ and $c = \mathrm{dot}\left[(\mathbf{ta}),(\mathbf{n})\right]$.

3.6   Depths of Cut Calculation

Depths of cut can be calculated using discrete methods such as Z-map, Z-buffer and Octree. The main benefit of those is the applicability on very complex workpiece geometries where abrupt changes on the surface are seen. In those methods, calculation accuracy and time are compromised. In most of the sculptured surface geometries, abrupt changes are not observed. In addition, surface and workpiece information can easily be obtained analytically by the help of the recent developments in 3-D CAD systems. Due to these reasons, depths of cut are calculated by analytical methods. CC point and the surface normal are obtained from the reference file, and the rough geometry information of the workpiece is obtained from the CAD system.

3.6.1 Axial Depth of Cut Calculation

It must be noticed that the stock material in general differs in roughing and finishing operations, thus different cases are taken into account. In Figure 3-7, stock material amount for different process steps on a bumped surface is illustrated. Axial depth of cut is calculated by considering tool axis coincident with stock surface normal (rn). Axial depth of cut is defined as the distance between the stock surface and the tool position along the stock plane normal as shown in Figure 3-6, points P1, P2 and P3 defines the rough surface as a plane. Axial depth of cut is the distance between the given points P4 and P6 where, P6 is the intersection point of the rough surface and the imaginary line coincident with the rough surface normal (**rn**). P_4 and P_5 are the two points defining the imaginary line, and derived using CL point, tool axis (**ta**) and tool radius (r) as follows.

$$C = CL + r.(\mathbf{ta}) \tag{3.12}$$

$$P_4 = C - r.(\mathbf{rn}) \tag{3.13}$$

$$P_5 = P_4 + (\mathbf{rn}) \tag{3.14}$$

The main issue is the calculation of the intersection point, i.e. P_6. Using the line-plane intersection analysis [35] P_6 can be determined by solving the general plane equation and the line equations simultaneously. Equation of the plane passing through P1, P2 and P3 is given below [35]:

$$\begin{vmatrix} x & y & z & 1 \\ x_1 & y_1 & z_1 & 1 \\ x_2 & y_2 & z_2 & 1 \\ x_3 & y_3 & z_3 & 1 \end{vmatrix} = 0 \tag{3.15}$$

Similarly, the parametric equation of the line passing through P_4 and P_5 is given as follows.

$$\begin{aligned} x_6 &= x_4 + (x_5 - x_4)t \\ y_6 &= y_4 + (y_5 - y_4)t \\ z_6 &= z_4 + (z_5 - z_4)t \end{aligned} \tag{3.16}$$

$$P_i = \begin{bmatrix} x_i \\ y_i \\ z_i \end{bmatrix}, i = 1, 2, ..., 6 \,.$$ Simultaneous solution of (3.15) and (3.16) gives (t).

$$t = \frac{\begin{vmatrix} 1 & 1 & 1 & 1 \\ x_1 & x_2 & x_3 & x_4 \\ y_1 & y_2 & y_3 & y_4 \\ z_1 & z_2 & z_3 & z_4 \end{vmatrix}}{\begin{vmatrix} 1 & 1 & 1 & 0 \\ x_1 & x_2 & x_3 & x_5 - x_4 \\ y_1 & y_2 & y_3 & y_5 - y_4 \\ z_1 & z_2 & z_3 & z_5 - z_4 \end{vmatrix}} \tag{3.17}$$

This value is substituted back into (3.16) to calculate the point of intersection, P6. Finally, axial depth of cut is calculated as the distance between P4 and P6 as follows.

$$(a) = \left| \mathbf{P_4 P_6} \right| = \sqrt{(x_6 - x_4)^2 + (y_6 - y_4)^2 + (z_6 - z_4)^2} \tag{3.18}$$
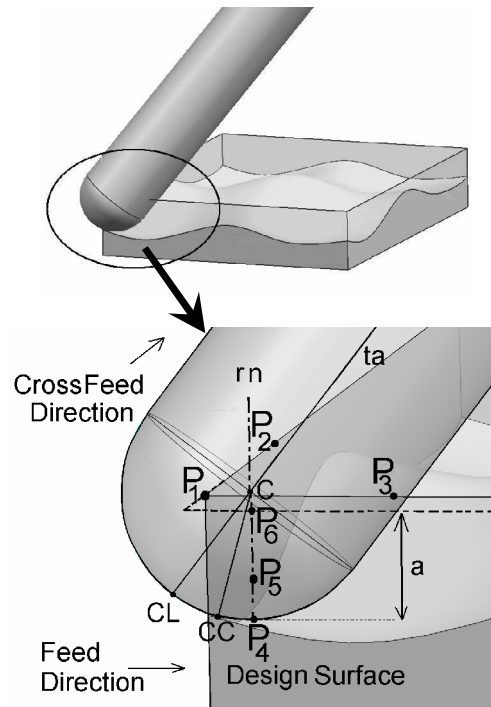
Figure 3-6: Calculation of (a)
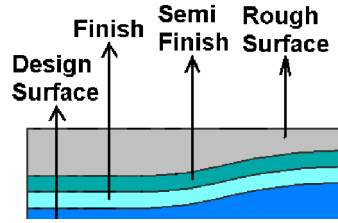
Figure 3-7: Difference of stock material

3.6.2 Radial Depth of Cut Calculation

As in the case of axial depth of cut, different should be considered in calculation of radial depth of cut. For example, (r) is different in the first cut step and the other cut steps as shown in Figure 3-8. In the first cut step, (r) is seen to be the distance from point RP1 to RP2 in Figure 3-9a. RP1 is the intersection point of (c) and tool envelope at that cross section. RP2 is the intersection point of (c) and the side surface.

$$(r) = \left|\mathbf{RP_1RP_2}\right| = \sqrt{(x_2 - x_1)^2 + (y_2 - y_1)^2 + (z_2 - z_1)^2} \tag{3.19}$$

where $RP_i = \begin{bmatrix} x_i \\ y_i \\ z_i \end{bmatrix}, i = 1, 2$

RP1 is calculated as follows and RP2 is similar to (3.16).

$$RP_1 = P + a.(\mathbf{n}) + R_a.(\mathbf{c}) \tag{3.20}$$

In the following cutting steps, (r) is taken to be the step size of the tool, which is defined as the distance from point $CC_{1,k}$ to $CC_{2,k}$ along the crossfeed vector as shown in Figure 3-9b. In this case radial depth of cut is calculated using the corresponding CC points at the consecutive cut steps as follows.

$$(r) = \left|(CC_{1,k} - CC_{2,k}).(c)\right| \tag{3.21}$$
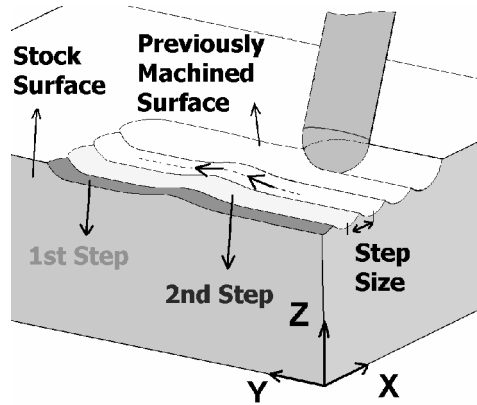
Figure 3-8: Illustration of cut steps

(a)   (b)
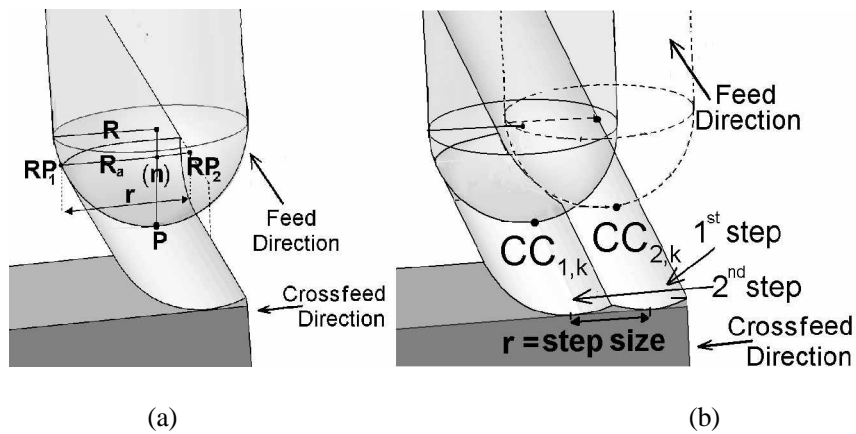
Figure 3-9: Calculation of (r)

3.7 Summary

In this chapter, calculation methodologies for FCN coordinate system and the geometrical parameters are presented. Surface normal vector which is needed to establish the FCN is obtained by a generated reference CL file. After calculating feed vector between consecutive CC points, cross feed vector is calculated by cross multiplication of the surface normal and the feed vectors. Lead and tilt angles are calculated using matrix transformation. Moreover, in calculation of depths of cut, different cases are observed in the first and other cut steps. In order to calculate depths of cut, the tool position must be known together with workpiece geometry.

26

Chapter 4

Verification of Geometrical Analysis Methods & Process Simulation

4.1   Introduction

In order to meet the increased demand for part quality in manufacturing environments, it is required to prevent undesired results such as high cutting forces and tool breakages. For this purpose, the process planner should have insight into the process beforehand. At this point, process simulation comes into consideration. By the help of process simulation, cutting forces can be estimated and counter action can be taken by the process planner. For such a purpose process model is integrated with the geometrical model. In this section, the proposed methods are applied on example tool paths and workpiece geometries. After the geometrical analysis methods are verified, process simulation technique is presented and verified by machining experiments. Tool paths are generated using the CAM software Unigraphics NX 3.0 © [36]. In the first example the methods are applied on machining of an airfoil surface given in Figure 4-10. The next example is machining of a complex surface. Calculated geometrical parameters and the exact values obtained from the CAD package are compared.

4.2   Example 1: Machining of an Airfoil Surface

In this example, the proposed methods are applied on an airfoil shaped surface, which is shown in Figure 4-1. Toolpath is generated under conditions given in Table 4-1. Machining is performed in two passes, i.e. rough and finish. The geometrical parameters at each point along the toolpath are calculated, and the variation of the extracted geometrical values along the toolpath is plotted.
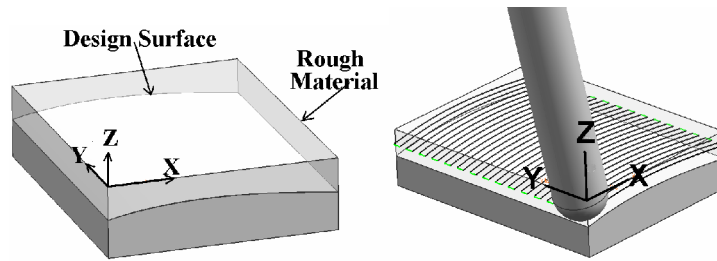
Figure 4-1: Surface to be machined in case 2.

	Rough	Finish
Tool Diameter	8 mm (ball-end)	8 mm (ball-end)
Tool Axis	Lead =8, Tilt=5 deg.	Lead =12, Tilt=3 deg.
Scallop Height	0.05 mm	0.005 mm
Left Stock	2 mm	0 mm
Passes	1	1
Points per Step	100	150
Cut Pattern	Linear / Zig	Linear / Zig

Table 4-1: Machining parameters for example 1.

In this example, the number of steps is decided considering the scallop height left on the surface. One way (Zig) cut pattern is applied on the surface. In order to keep an acceptable level of accuracy, relatively high number of points per step is chosen. In addition, 2 mm of stock material is left for the finish pass on the design surface. The toolpath is presented in Figure 4-1. In Figure 4-2 to Figure 4-9 calculated parameters along the toolpath are plotted.

In Figure 4-2, the variation of axial depth of cut is shown. It is at the maximum level (2.2mm) at the start and end of each step and minimum (0.98 mm) at the middle of each step. For the finish pass, axial depth of cut is constant (2 mm).

Figure 4-2: Variation of axial depth of cut in roughing.
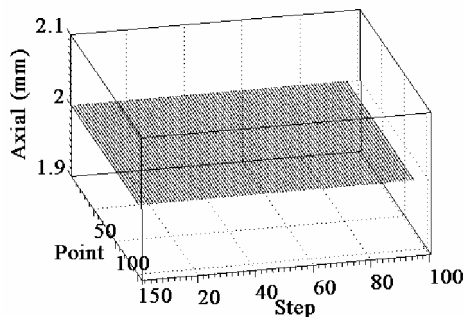
Figure 4-3: Variation of axial depth of cut in finishing.

Radial depth of cut changes with the position of the tool at the first and the last steps, and it remains constant along other steps. At first and last steps, the tool machines the flat side of the rough material. Thus, radial immersion is relatively higher with respect to other steps. In finishing pass, since the stock on the surface is constant the radial depth of cut does not vary along the first and last steps.

Figure 4-4: Variation of radial depth of cut in roughing.

29
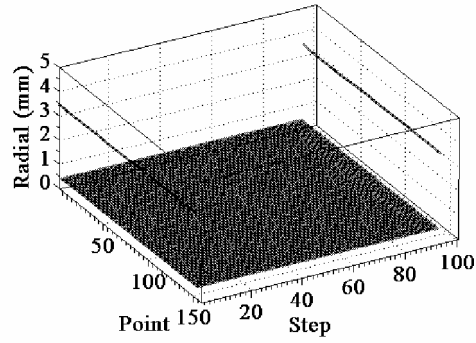
Figure 4-5: Variation of radial depth of cut in finishing.

Lead and tilt angles are calculated accurately as seen in the following figures. The calculated values are around the nominal values with tight tolerances.

Figure 4-6: Calculated lead angle for roughing (nominal 8 deg).

Figure 4-7: Calculated lead angle for finishing (nominal 12 deg).

30
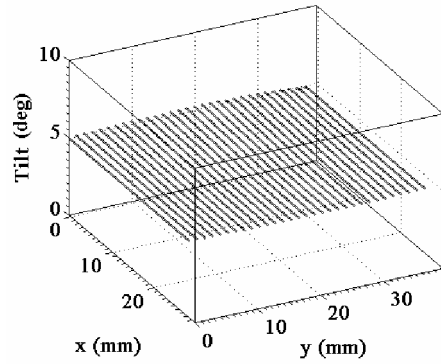
Figure 4-8: Calculated tilt angle for roughing (nominal 5 deg).

Figure 4-9: Calculated tilt angle for roughing (nominal 3 deg).

4.3   Example 2: Machining of a Free Form Surface

In this example, geometrical analysis and modeling methods are applied on machining of the complex surface shown in Figure 4-10. Machining is performed in two steps, i.e. rough and finish. Finishing is performed in 2 passes. Zig-zag cut pattern is applied where the process parameters are given in Table 4-2.
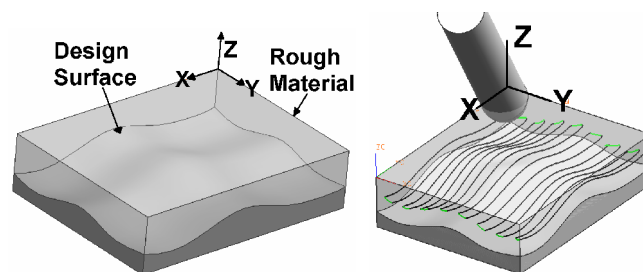
Figure 4-10: Surface for example 2

31

	Rough	Finish
Tool Diameter	6 mm (ball-end)	6 mm (ball-end)
Tool Axis	Lead =15, Tilt=5 deg.	Lead =10, Tilt=5 deg.
Scallop Height	0.1 mm	0.02 mm
Left Stock	2 mm	0 mm
Passes	1	2
Points per Step	150	200
Cut Pattern	Linear / Zig-Zag	Linear / Zig-Zag

Table 4-2: Machining parameters for example 2.

Number of steps is decided considering the scallop height left on the surface. For this case two way (Zig-Zag) cut pattern is applied on the surface. Since the surface has more complex characteristics higher number of points per step is chosen. 2 mm of stock material is left on the design surface for finish pass. Finishing pass is performed in 2 passes. The toolpath is presented in Figure 4-10.

In Figures 8.11 – 8.18 calculated parameters along the toolpath are plotted as in example 1. Axial depth of cut continuously varies along each step and also among the steps. At five positions of the tool along the 1st step, the axial depth of cut values are compared with the values directly measured from the CAD software. The comparison is given in Table 4-3.

Position (mm)	Axial (mm)	
	Measured	Calculated
1)X=0.016,Y=0.013	2.96	2.96
2)X=11.490,Y=0.296	2.02	2.02
3)X=14.760,Y=0.448	1.36	1.36
4)X=25.920,Y=0.001	3.53	3.53
5)X=28.190,Y=0.013	3.13	3.13

Table 4-3: Measured and Calculated Axial Depth of Cut Values.
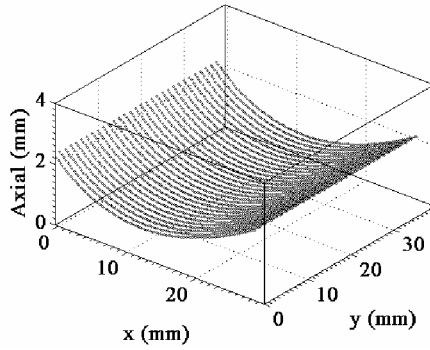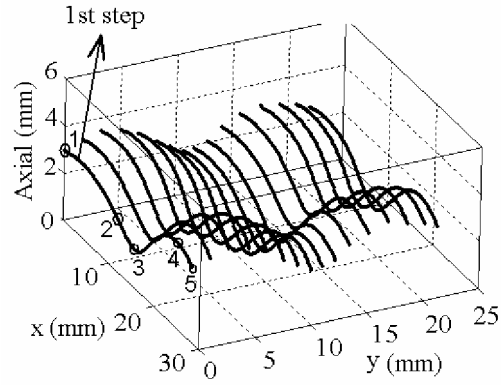
Figure 4-11: Variation of axial depth of cut in roughing.
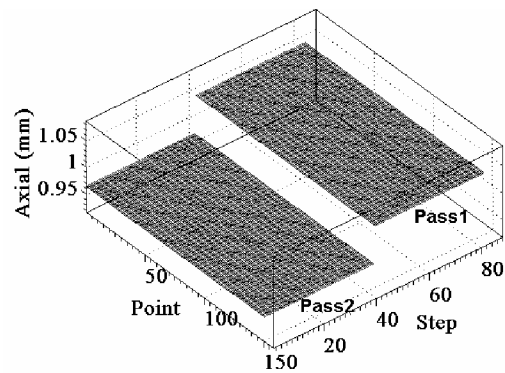
Figure 4-12: Variation of axial depth of cut in finishing.

Since the surface has complex characteristics both in u-v directions, the distance between the steps varies on the surface. This is to generate uniform scallop distribution on the surface. Consequently the variable radial depth of cut varies along steps contrarily to the first example. At first and last steps, the tool cuts flat side of the rough material. Thus, radial immersion is relatively higher with respect to other steps.
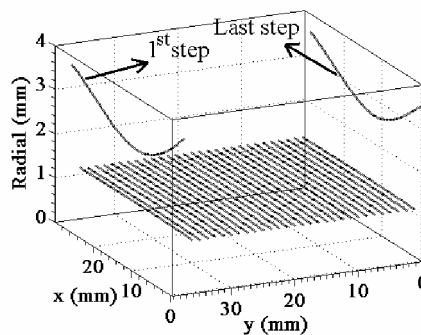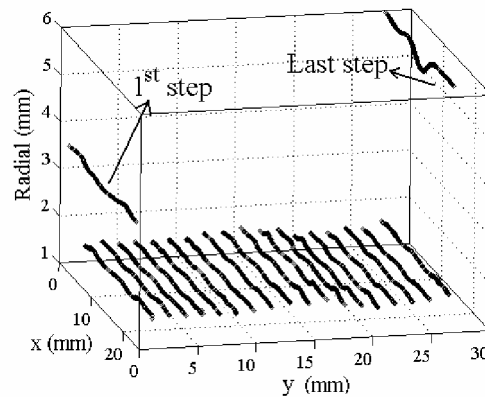

Figure 4-13: Variation of radial depth of cut in roughing.

33
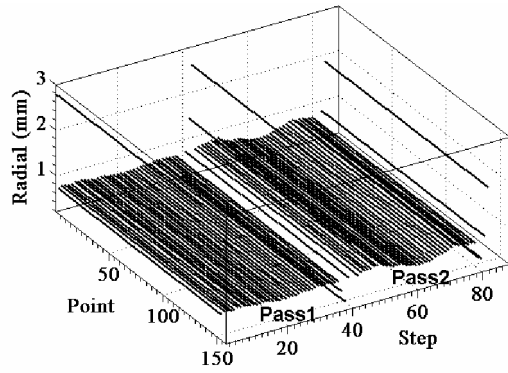
Figure 4-14: Variation of radial depth of cut in finishing.

As seen in Figure 4-15 to Figure 4-18 lead and tilt angles are calculated accurately. The maximum error is about 0.5 degrees for lead angle and 0.15 degrees for tilt angle.
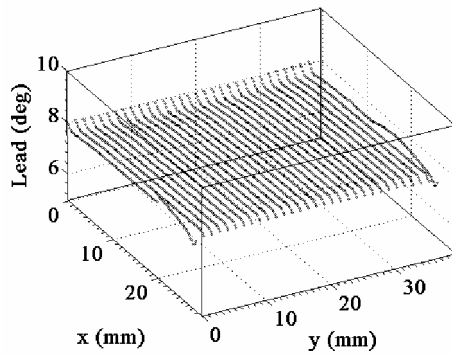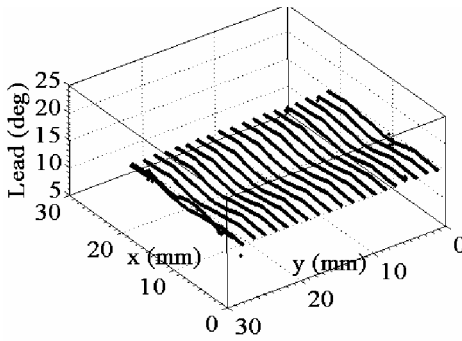

Figure 4-15: Calculated lead angle in roughing (nominal 15 deg).
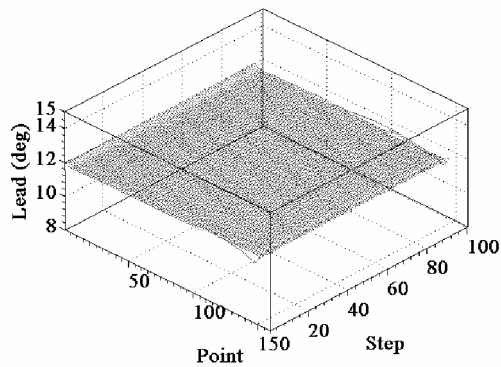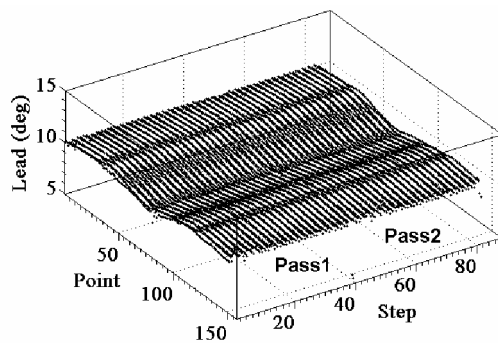

Figure 4-16: Calculated lead angle in finishing (nominal 10 deg).

34

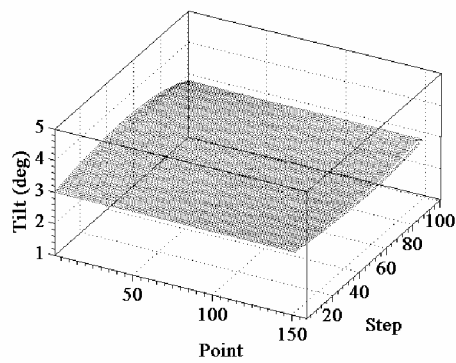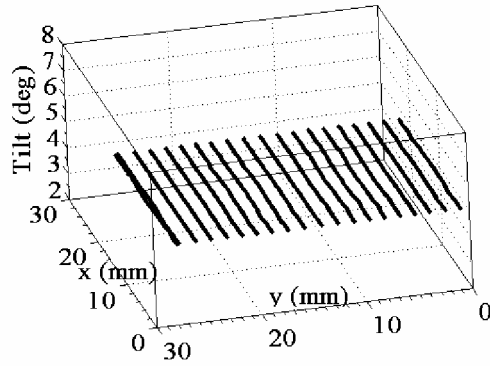Figure 4-17: Calculated tilt angle in roughing (nominal 5 deg).
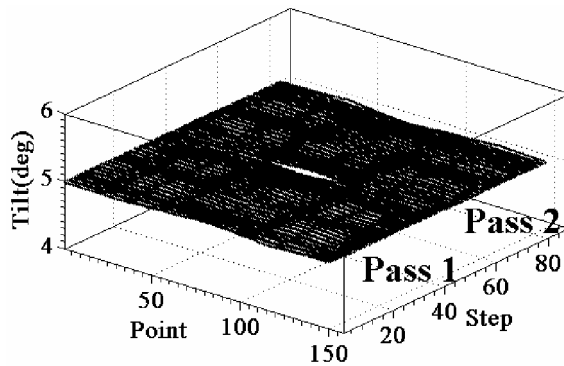
Figure 4-18: Calculated tilt angle in finishing (nominal 5 deg).

4.4 Process Simulation Methodology

In the literature, two simulation approaches are considered to serve different purposes. In the first approach, desired machining conditions are simulated individually to have an insight into the process mechanics under different conditions. By doing so, some guidelines, e.g. selection of best combination of lead and tilt angles, may be provided to the process planner beforehand. The second approach considers a whole process where machined surface topology and cutting conditions vary continuously. In this approach, mechanics of the process is simulated along the tool path to predict the variation of forces throughout the process. Thus, undesired results can be prevented and process can be improved or optimized. Besides, feed rate scheduling can be applied in order to keep the cutting forces below a desired level. This may be beneficial to decrease machining time while preventing the tool from being subjected to high cutting forces.

35

In this thesis, the second approach is performed in the following manner. Geometrical parameters are calculated at each or desired points throughout the toolpath. Once depths of cut and lead-tilt angles at each point are determined, they are used in the force model [26]. By doing so, force simulation is performed for one revolution of the tool at each point and forces are obtained as in Figure 4-19 . Finally, the maximum value of forces in each direction is plotted. Hence, variation of the maximum cutting forces along the toolpath is simulated. Process simulation procedure is summarized in Figure 4-20.
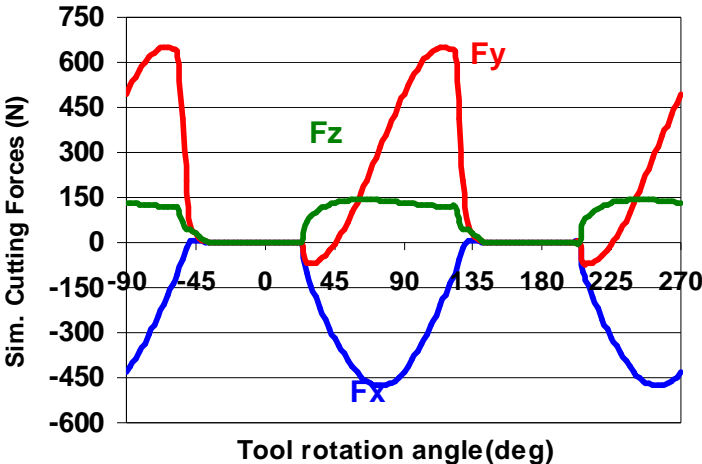
Figure 4-19: Forces for one revolutions of tool.
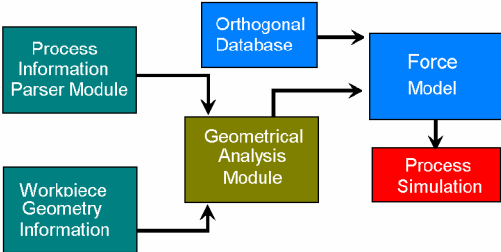
Figure 4-20: Simulation procedure.

4.5   Experimental Verification & Simulation Results

Applicability of the proposed method is verified by machining experiments. As an example, the surface given in Figure 4-21 is machined. The forces along the first cut

step is measured and simulated. Results are compared in Figure 4-22. Experiment parameters are given in Table 4-4.
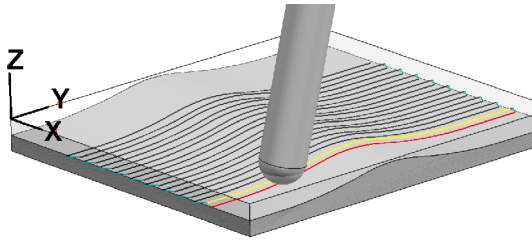
Figure 4-21: Machined surface in experiments

Side Step (mm)	1
Spindle Speed(rpm)	3000
Feed (mm/rev/tooth)	0.1
Lead (deg)	[-10,..10]
Tilt (deg)	0

Table 4-4: Experiment conditions.
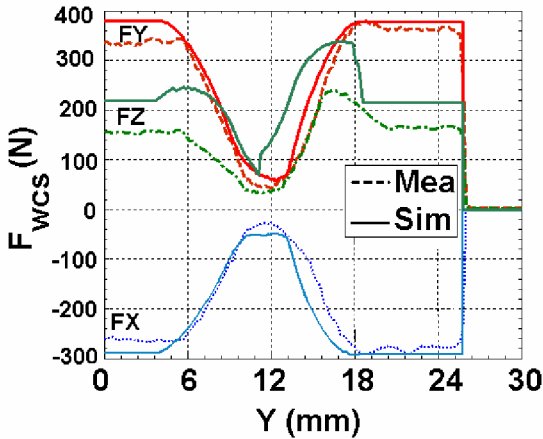
Figure 4-22: Simulated and measured cutting forces

As seen in Figure 4-22 measured and simulated forces in X-Y-Z directions show acceptable agreement. However, some discrepancy is seen in the force in Z direction. This is due to the indentation forces created at the tool tip where the cutting edge can not cut to due to the fact that the cutting speed reduces to zero at the center. However, these forces can also be identified and included in the ball end milling model which is currently an on going research in our laboratory.

4.6 Summary

In this chapter, the methods proposed in the previous chapter are applied on two different surface geometries and the results are given. Smooth variation is seen in calculated axial depth of cut values in rough passes. In addition, the difference in radial depth of cut between the first cut and the following cut steps are seen obviously. Lead and tilt angles are calculated in acceptable tolerances around the given nominal values. In addition, process simulation methodology is presented. The methodology is verified by machining of a bumped surface. The simulated and measured cutting forces are compared. A good agreement between simulated and measured values is seen. However, some amount of discrepancy is observed in forces in Z direction. Thus, it can be concluded that the proposed methods are applicable to analyze 5-axis milling geometry of regular sculptured surfaces. Moreover, by integrating the process model with the geometrical analysis methods, cutting force simulation of a given process can be performed.

Chapter 5

Process Optimization

5.1   Introduction

Increasing productivity and part quality are the main challenges in machining industry. From process mechanics point of view, productivity may decrease due to undesired results such as tool breakage or excessive form errors. This may occur due to high cutting forces if the process parameters are not selected properly. In order to overcome such problems, either an existing process may be improved or optimized parameters may be provided to the process planner beforehand. For such purposes, machining parameters such as feed rate, depths of cut and tool orientation may be optimized considering the process mechanics. Effect of those named parameters on the process mechanics can be investigated experimentally or by using process models.

Applying the appropriate machining strategy is of great importance. This is because of the fact that machining time, surface quality and texture, tool trajectory on the surface and variation of the cutting forces along the trajectory directly depend on the applied machining strategy. Thus, the best strategy for a given surface should be investigated. The geometry and mechanics of such processes are complicated; therefore models should be constructed for such a purpose. There are mainly two objectives; the first one is proposing a new strategy and latter is selection of the most appropriate strategy among various existing default strategies such as the ones available in CAM system.

Milling operations are performed generally in two passes which are finishing and roughing. Requirements for each type of operation are different. In roughing relatively high cutting forces occur and the resulting surface quality is not so important resulting in higher material removal rate. The aim is removing as much material as

possible while preventing excessive cutting forces. On the other hand, finishing requires high surface quality. Therefore, appropriate machining strategy should be evaluated with respect to different criteria for each type of operation. In this study, process mechanics and the surface characteristics are considered together with machining time for roughing and finishing, respectively. Though, since the process optimization is based on process simulations, the proposed methods do not guarantee the global optimal conditions.

5.2   Optimization of tool orientation

In literature, there are important studies on optimization of tool orientation [24], [4]. Effect of feed rate and other parameters on process mechanics and part quality is quite obvious. On the other hand effect of tool orientation i.e. lead and tilt angles, is not that obvious. In most of the cases, even when other cutting parameters are known, selection of lead and tilt angles is an important challenge in 5-axis milling. It is not straight forward to choose optimal lead and tilt angles due to many possible combinations and their non-linear effects on the process mechanics. Therefore, foresight about the effect of those on the process mechanics is required in order to select appropriate values.

In this thesis, the effect of lead and tilt angles on the process mechanics is investigated under different machining conditions in order to provide a general idea. This is performed in the following manner. Under various radial depths of cut, forces are simulated in a range of lead-tilt angle combinations using the existing force model [26]. Variation of the maximum resultant force in the transversal direction along the tool axis, F_{xy}, (see Figure 5-2) is plotted as a surface among the lead-tilt angle combinations as shown in Figure 5-3. Finally, the combination which leads the minimum value of the force, F_{xy}, is selected as the optimum combination. Optimization procedure is summarized in Figure 5-1.
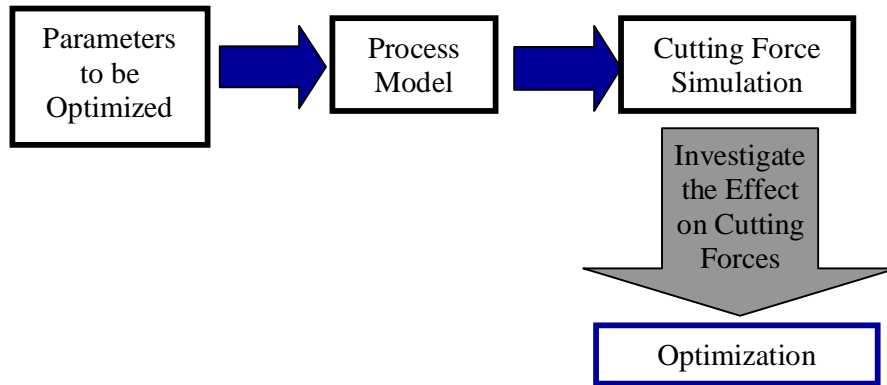
Figure 5-1: Orientation optimization procedure.
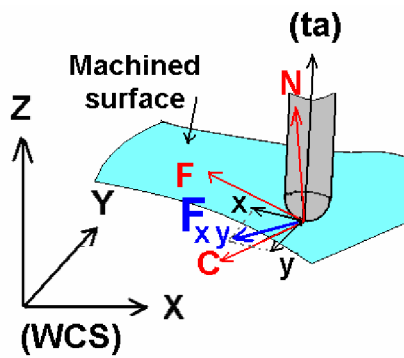
Figure 5-2: Representation of Fxy.
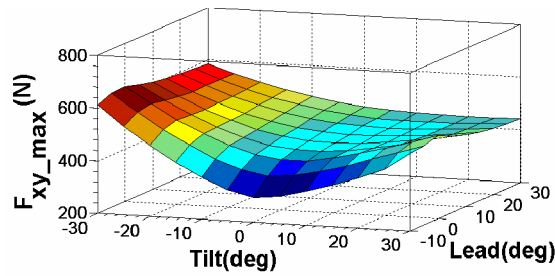
Figure 5-3: Variation of Fxy among lead-tilt combinations

By applying the proposed methodology, appropriate pairs of lead and tilt angles can be selected once other machining parameters are set. In order to verify the proposed approach, machining experiments are conducted. In the following section simulation and experimental results are compared.

5.2.1   Simulations Results and Experimental Verification

For various radial depths of cuts simulations are performed under conditions given in Table 5-1. In order to verify the simulation results machining experiments are conducted under various radial depth of cuts values. Simulation results and experimental results are presented in Figure 5-4 to Figure 5-8 and in Table 5-2 respectively. A 2 fluted, 12 mm diameter, carbide, ball-end mill is used in the experiments. For machining experiments three pairs of lead and tilt angles are selected for each case, where F_{xy} is at minimum, medium and high levels respectively. By doing so, also the estimation on the trend of F_{xy} is verified.

Spindle Speed(rpm)	3000
Feed (mm/rev/tooth)	0.1
Lead (deg)	[6,9..30]
Tilt (deg)	[-30,-27…30]
Axial depth (mm)	1.5
Local Radius, Ra (mm)	3.69

Table 5-1: Simulation & experiment conditions.
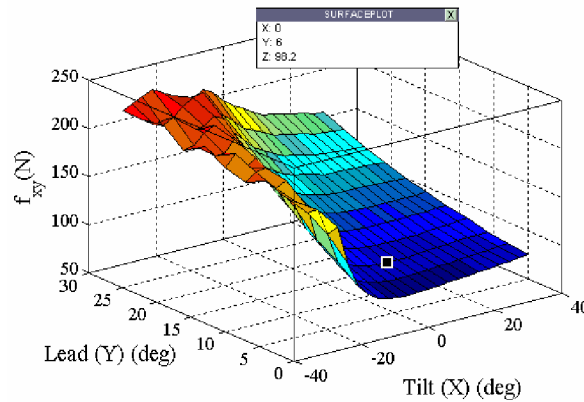
Figure 5-4: Variation of Fxy (r =1.2 mm)
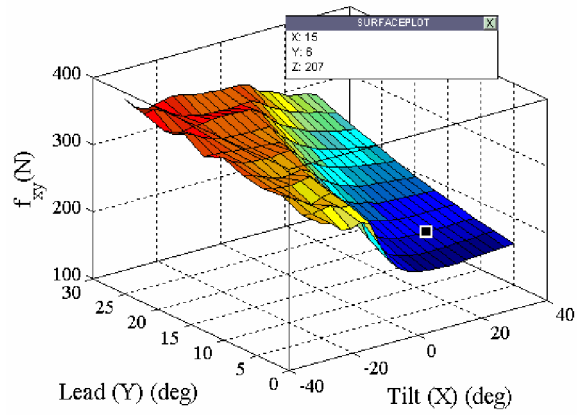
Figure 5-5: Variation of Fxy (r =2.4 mm)
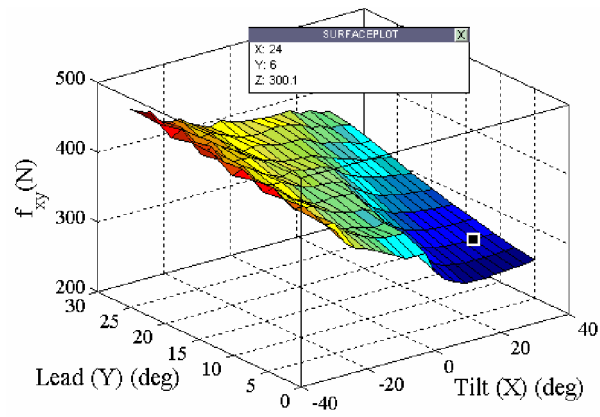
Figure 5-6: Variation of Fxy (r =3.6 mm)
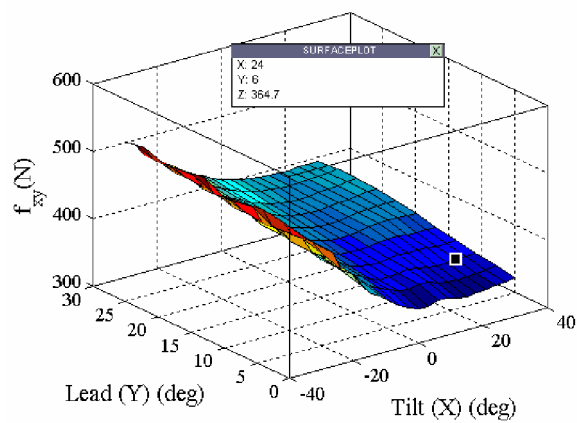
Figure 5-7: Variation of Fxy (r =4.6)

43
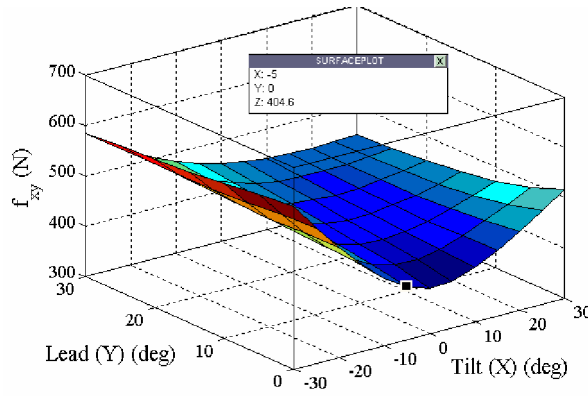
Figure 5-8: Variation of Fxy (r =slot)

Radial (mm)		1.2			2.4		
Lead (deg)		6	6	27	6	6	24
Tilt (deg)		0	-21	-12	15	-12	-27
Fxy,max (N)	Sim.	98	141	222	207	294	326
	Exp.	150	180	210	255	317	335

Radial (mm)		3.6			4.6		
Lead (deg)		6	6	24	6	6	18
Tilt (deg)		24	-6	-27	24	-15	-30
Fxy,max (N)	Sim.	300	357	444	365	410	495
	Exp.	310	405	440	385	420	460

Radial (mm)		Slot		
Lead (deg)		0	10	5
Tilt (deg)		-5	-15	-30
Fxy,max (N)	Sim.	404	479	620
	Exp.	450	500	630

Table 5-2: Experimental v simulation results.

In the simulation results it is seen that the optimal value of lead angle does not show significant change by radial depth of cut. On the contrary, optimum value of tilt angle changes with radial depth of cut. Until the half immersion of the tool, the optimum value of tilt angle increases, and then decreases as radial depth of cut exceeds half immersion. In general, experiments show good agreement with the simulations results. Some discrepancy is observed between the measured and simulated cutting forces for low radial depth of cut values.

5.3   Optimization of Other Machining Parameters

Machining operations are subject to several limitations which are cutting torque, cutting power, tool breakage, tool deformation, and chatter vibrations. In addition the tool life should be longer than the operation time since it is not preferred to change tool during the operation. This may decrease the resulting workpiece quality. Therefore, other machining parameters such as feed rate, cutting speed, and depths of cut should be compromised such that total machining time is minimized. Those parameters have non linear effect on process mechanics. Moreover, there is not an analytical process model to simulate cutting forces for 5-axis milling processes. Thus, most of the non linear optimization methods are not applicable to such processes.

In this thesis, a method is proposed to minimize the total machining time of a roughing process by compromising between the named machining parameters. Total machining time is given as follows;

$$(TMT) = (NOP)*(TPP) \tag{5.1}$$

where, TMT is the total machining time, NOP is the number of passes, and TPP is machining time per pass. The chosen machining parameters should satisfy the below conditions,

i.   Process should be stable under chosen axial and radial depths of cut and cutting speed.

ii.   Chosen feed per tooth (fpt) should be less than maximum available feed per tooth for a given tool.

iii.   Maximum stress on the tool should not exceed tool rupture stress

iv.   Required cutting power and torque should not exceed available torque and power on the spindle.

v.   Tool life must be greater than the machining time.

The steps of the proposed method are given in Figure 5-9. Once the tool geometry is determined, CL file with small axial increments and radial step over is generated in order to calculate machining time for a given pass at future steps. Since the tool is assumed to be more flexible than the workpiece in roughing operations machine tool dynamics are measured. Pairs of stable axial and radial depths of cut, i.e. a_{lim}, b_{lim}, are obtained using the methodology proposed by Tekeli et al. [30] where, b= r / 2R It may not lead to minimum machining time to directly use obtained a_{lim}, b_{lim} values with a

45

given feed per tooth(fpt). Thus, it may be required to search for better fpt for each pair. So, the obtained pairs of stable depths of cut values are used as initial values to search feasible fpt, a, b values. For such a purpose a search algorithm is developed considering the limitations mentioned previously for given initial a_{lim}, and b_{lim} values. The pseudo codes of developed algorithms are given in Figure 5-10 and Figure 5-11.

Determine Tool Geometry, d_t, l_t	→	Generate CL file with small increments of axial and radial depth of cuts	→	Measure Machine tool Dynamics

Choose a, b, fpt to minimize (TMT) = (NOP)*(TPP)	←	Obtain feasible fpt, a, b values.	←	Obtain stable a vs. b pairs for given RPM
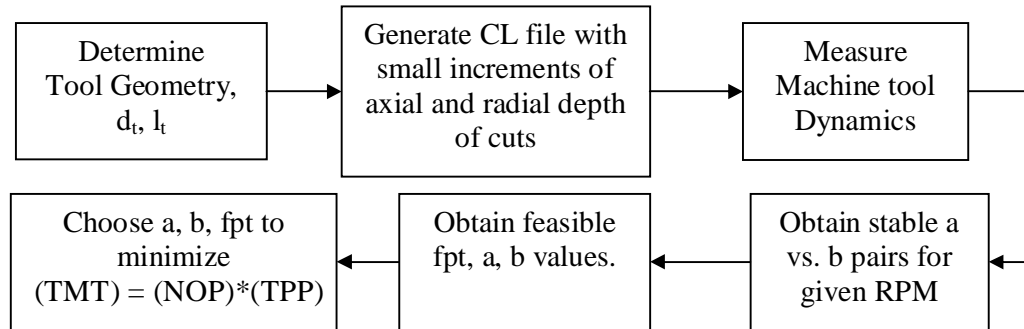
Figure 5-9: Overview of the proposed method.

```
Obtain "spindle speed" and stable "alim vs. blim" pairs.
FOR pair=1: number_of_pairs

    Set fpt fpt_max
    ok=0
    WHILE ok=0

        Calculate cutting Force, Torque, Power, Tool Stress, and Deflection
        Torque ratio = Torque available / Calculated Torque
        Power ratio = Power available / Calculated Power
        Stress ratio = Tool Rupture Limit / Calculated Stress
        Deflection ratio = Deflection Limit / Calculated Deflection
        Min ratio= min (Torque, Power, Stress, Deflection ratio)

        IF Min_ratio>1 & fpt=fpt_max THEN
            feasible_max_fpt (pair) =fpt
            ok=1
        END IF
        IF Min_ratio < 1 & fpt > min. available fpt THEN
            fpt=exp (1.2*(min_ratio-1))*fpt
        ELSE IF fpt<min. available fpt THEN
            feasible_max_fpt (pair)=0;
            ok=1
        END IF
        IF 1.05>Min_ratio>1 & fpt<fpt_max THEN
            feasible_max_fpt (pair) =fpt
            ok=1
        END IF
        IF Min_ratio>1.05 & fpt<fpt_max THEN
```

```
                fpt=exp (1.2*(min_ratio-1))*fpt
        END IF

    END WHILE
    Calculate MRR (pair)
NEXT pair
```

Figure 5-10: Pseudo code for max feasible feed rate determination.

```
Set mean_MRR=average of MRR (pairs)

FOR pair=1:number_of_pairs
    IF MRR (pair)>=mean_MRR
        Initialize machining_time(pair)=0

        Calculate tool life
        Calculate linear feed rate = rpm(pair) * feasible_fpt(pair)*teeth
        number_of_passes=ceil(depth/axial)
        FOR pass=1:number_of_passes
            Calculate the machining time for the corresponding axial layer
        NEXT pass
        Update machining_time(pair)

    END IF
NEXT pair

Choose the pair with minimum total machining time.
Compare the operation time with the tool life at that cutting speed.
```

Figure 5-11: Pseudo code for minimum machining time determination

5.4   Machining Strategy Evaluation and Selection

In evaluation various strategies on free form surfaces, surface information should be obtained from the CAD software. In this thesis, surface is represented in Bezier surface form which is defined by equation (5.2). Pole point coordinates and surface information in u-v directions are obtained from CAD software (see Figure 5-12).

$$P(u,v) = \sum_{i=0}^{n} \sum_{j=0}^{m} P_{i,j} B_{i,n}(u) B_{j,m}(v) \qquad (5.2)$$

where;

$$B_{i,n}(u) = \binom{n}{i} u^i (1-u)^{n-i}$$

$$B_{j,m}(v) = \binom{m}{j} v^j (1-v)^{m-j}$$
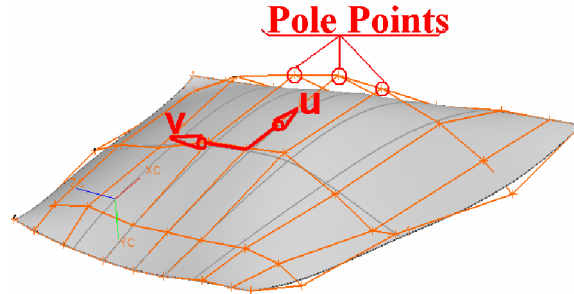
Figure 5-12: Pole points of a Bezier surface

5.4.1 Machining Strategy Evaluation for Roughing

Material removal rate is high in roughing operations and cutting tool is exposed to relatively high forces. Thus, primarily process mechanics should be taken into the consideration in strategy evaluation and selection. In addition, high variation in the cutting forces is not desired. Therefore, magnitude and variation of forces is taken into account.

5.4.1.1 Proposing a New Strategy

In some cases, a new strategy or cutting direction other than the default ones is needed. So, it is required to investigate for a new strategy or cut direction. For such a purpose, the procedure summarized in Figure 5-13 is followed. Firstly, control points are selected on the surface in u-v range as shown in Figure 5-14. At each control point, P_{uv}, force simulation is performed along several local cutting directions $d(\theta)$ and at the point P_{uv} itself. According to the simulation results, the penalty function is calculated for each local direction and the direction with minimum penalty value is selected as the local direction at point P.
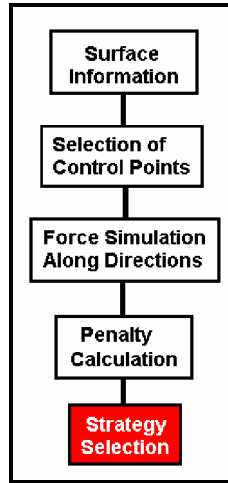
Figure 5-13: Machining strategy selection procedure.

The penalty function is defined as follows:

$$Dir\_Penalty(d) = w_M.F_{mag}^{P,d}(d) + w_D.F_{dev}^{P,d}(d) \tag{5.3}$$

where;

w_M: Weight of the force magnitude

w_D: Weight of the force deviation

$F_{mag}^{P,d}(d)$: Magnitude of the force at point $P_{u,v}^d$

$F_{mag}^{P,d}(d) = \left| F_{mag}^P - F_{mag}^{P,d} \right|$

$0 < w_M < 1$ and $w_M + w_D = 1$
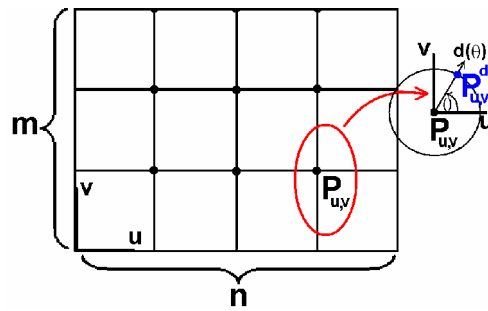
Figure 5-14: Control points in u-v range.

$$d(\theta) = \begin{bmatrix} du \\ dv \end{bmatrix} = \begin{bmatrix} \dfrac{\cos\theta}{k.\max(m,n)} \\ \dfrac{\sin\theta}{k.\max(m,n)} \end{bmatrix} \tag{5.4}$$

By use of such an approach, forces are kept under a desired level while preventing high deviations along the machining direction. This methodology is applied on different surface geometries and the results are presented in the following chapter.

5.4.1.2 Comparison of Given Strategies

Recent CAM software offers various milling strategies by default. Generally, it is a big challenge to decide the right strategy in CAM programming. Therefore, the machining strategies provided by the CAM software should be compared and the appropriate strategy should be identified. For such a purpose, the given strategies should be compared from process mechanics and machining time aspects.

5.4.1.2.1   Process Mechanics

In comparison of given strategies an approach similar to the one presented in the previous section is followed. Control points are created with respect to the considered strategy pattern as shown in Figure 5-14. Global machining directions are applied on each control point and local directions are determined as shown in Figure 5-15. At each point itself and along the local directions, geometrical parameters are calculated and a force simulation is performed. Then, penalty function at each control point is calculated with respect to force magnitudes and variations as follows:

$$\text{Pt\_Penalty(p)} = w_M . F_{mag}^P + w_D . F_{dev}^D \tag{5.5}$$

where,

$$F_{dev}^P = abs(F_{dev}^P - F_{dev}^{P\text{-}1}) \text{ for } p > 1$$
$$F_{dev}^P = 0 \text{ for } p = 1$$
S

Finally, total penalty due to forces is calculated as follows,

$$F\_Penalty = \sum_{p=1}^{C} Pt\_Penalty(p) \tag{5.6}$$

where, C denotes total number of control points.
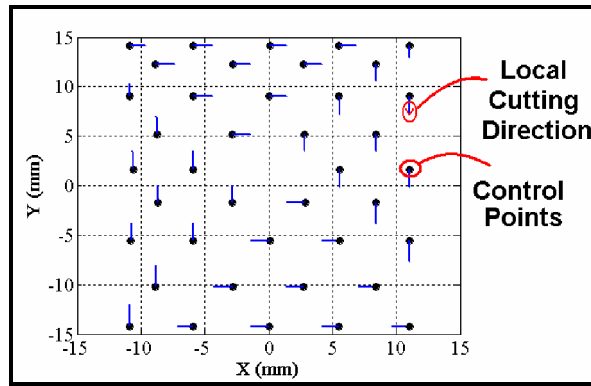
Figure 5-15: Local directions at control points

5.4.1.2.2   Machining Time Comparison

Besides the cutting forces, machining time is another criterion in strategy selection. Moreover, in some cases it may be the most important criterion. Thus, machining time should be calculated for a given surface and strategy pair, and must be taken into consideration together with the penalty due to cutting forces.

For given machining strategy and machining conditions, machining time calculation procedure is summarized in Figure 5-16. Desired number of points per each cut step is created on the surface with respect to the machining strategy pattern. Incremental distance between consecutive points along the cut steps is calculated as follows:

$$dp = \left| P_{i,j} P_{i,j+1} \right| = \sqrt{(P^x_{i,j+1} - P^x_{i,j})^2 + (P^y_{i,j+1} - P^y_{i,j})^2 + (P^z_{i,j+1} - P^z_{i,j})^2} \tag{5.7}$$

All incremental distances are summed for each step to calculate the toolpath length. Path length for rapid and feed moves is calculated separately where clearance, step over and retract moves are considered as rapid. In addition, step size of the tool is pre defined.
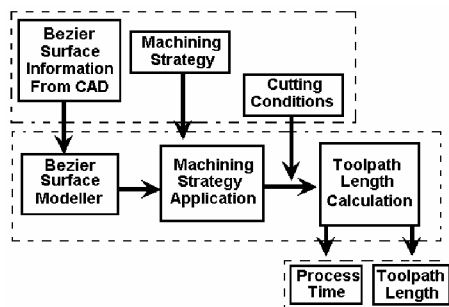
Figure 5-16: Machining time calculation procedure
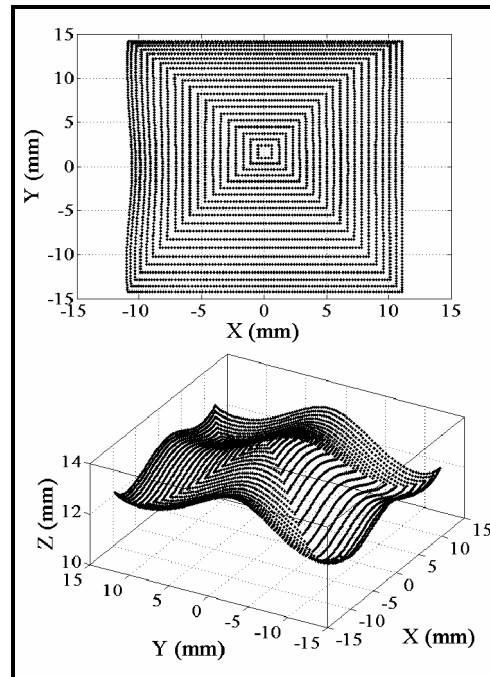
Figure 5-17: Points on the surface

After calculating the total force penalty and the machining time, the strategy which has minimum overall weighted penalty with respect to cutting forces and machining time is selected.

5.4.2   Strategy Evaluation for Finishing Operations

Contrary to roughing, material removal rate is low in finishing operations and the cutter is not subjected to high cutting forces. Besides, resulting surface quality is of great importance in finishing. Sculptured surfaces are bounded by edges. However, those define its parametric coordinates. Surface characteristics are related to its intrinsic properties at any point (see Figure 5-18). Those intrinsic properties can be named as, the surface normal, curvature etc. In conventional methods, one of the edges is chosen as the master cutter path and the other steps are derived from that edge. By doing so, the tool trajectory becomes unrelated with surface characteristics. On the other hand, if the toolpath is derived with respect to the intrinsic properties, some machining parameters and the surface quality may be optimized. In the literature, it is reported that the machining time decreases when the cutting directions are chosen in the maximum

convex curvature direction [13]. This is because, larger side step can be applied for a given scallop height. Besides, it may be beneficial to evaluate machining strategies considering the tool deformations [17]. By doing so, machining error on the surface can be minimized. The methodology used for roughing operations can be used for this purpose. It is required to re-define the penalty function to be related to tool deflection. Moreover, maximum available tool diameter can be determined that can be used in machining of a given surface by knowing the intrinsic properties of the surface.
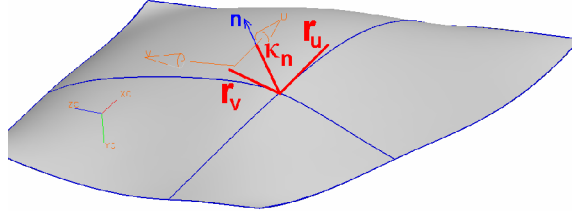
Figure 5-18: Representation of intrinsic properties

5.4.2.1 Mathematical Formulation

As mentioned previously, surfaces are represented in Bezier surface form. In this section, derivation of intrinsic properties is presented. Normal curvature in a direction $\dfrac{dv}{du}$ [13] is given as follows:

$$\kappa_n = \frac{d_{11} + 2d_{12}\left(\dfrac{dv}{du}\right) + d_{22}\left(\dfrac{dv}{du}\right)^2}{g_{11} + 2g_{12}\left(\dfrac{dv}{du}\right) + g_{22}\left(\dfrac{dv}{du}\right)^2} \qquad (5.8)$$

where, d_{ij} and g_{ij} are the elements of first and second fundamental forms, which are given below. In the following matrices $r_u, r_v, r_{uu}, r_{uv}, r_{vv}$ represent the partial derivatives. Derivations of the partial derivatives are given as follows:

$$G = \begin{bmatrix} g_{11} & g_{12} \\ g_{21} & g_{22} \end{bmatrix} = \begin{bmatrix} r_u r_u & r_u r_v \\ r_u r_v & r_v r_v \end{bmatrix} \text{ first fundamental form}$$

$$H = \begin{bmatrix} h_{11} & h_{12} \\ h_{21} & h_{22} \end{bmatrix} = \begin{bmatrix} r_{uu}.n & r_{uv}.n \\ r_{uv}.n & r_{vv}.n \end{bmatrix} \text{ second fundamental form}$$

$$(5.9)$$

First partial derivative of P(u,v) with respect to "u" and "v" leads to r_u and r_v respectively.

$$r_u = \frac{\partial P(u,v)}{\partial u} = \sum_{j=0}^{m} C_j B_{j,m}(v) \qquad (5.10)$$

$$r_v = \frac{\partial P(u,v)}{\partial v} = \sum_{i=0}^{n} C_i B_{i,n}(u) \qquad (5.11)$$

where

$$C_i = \sum_{j=0}^{m-1} \binom{m-1}{j} v^j (1-v)^{m-j-1} a_{0,j} \quad , \quad C_j = \sum_{i=0}^{n-1} \binom{n-1}{i} u^i (1-u)^{n-i-1} a_{i,0}$$

$$a_{0,j} = P_{0,j+1} - P_{0,j} \qquad\qquad a_{i,0} = P_{i+1,0} - P_{i,0}$$

Second partial derivatives of r_u and r_v with respect to "u" and "v" lead r_{uu}, r_{uv} and r_{vv}.

$$r_{uu} = \frac{\partial^2 P(u,v)}{\partial u^2} = \sum_{j=0}^{m} D_j B_{j,m}(v) \qquad (5.12)$$

$$r_{vv} = \frac{\partial^2 P(u,v)}{\partial v^2} = \sum_{i=0}^{n} D_i B_{i,n}(u) \qquad (5.13)$$

$$r_{uv} = r_{vu} = \frac{\partial^2 P(u,v)}{\partial v \partial u} = \frac{P(u,v)}{\partial v \partial u} = \frac{\partial}{\partial v}\left(\sum_{j=0}^{m-1} C_j B_{j,m}(v) \right) =$$

$$= \sum_{j=0}^{m-1} C_j \frac{\partial}{\partial v}\left(\sum_{j=0}^{m-1} B_{j,m}(v) \right) = \sum_{j=0}^{m-1} C_j \binom{m-1}{j} v^j (1-v)^{m-1-j} \qquad (5.14)$$

where,

$$D_j = \sum_{i=0}^{n-2} \binom{n-2}{i} u^i (1-u)^{n-i-2} b_{i,0} \quad , \quad D_i = \sum_{j=0}^{m-2} \binom{m-2}{j} v^j (1-v)^{m-j-2} b_{0,j}$$

$$b_{i,0} = a_{i+1,0} - a_{i,0} \qquad\qquad b_{0,j} = a_{0,j+1} - a_{0,j}$$

Finally, principal curvatures are obtained [8] as follows.

$$\kappa_{n_1} = \frac{(b + \sqrt{b^2 - 4ac})}{a}, \kappa_{n_2} = \frac{(b - \sqrt{b^2 - 4ac})}{a} \tag{5.15}$$

where,

$$
\begin{aligned}
a &= |G| \\
c &= |D| \\
b &= \frac{(g_{11}.d_{22} + g_{22}.d_{11})}{2} - g_{12}.d_{12}
\end{aligned} \tag{5.16}
$$

For the surface given in Figure 5-19, first and second principal curvatures are calculated. The calculated values are plotted in 2-D and 3-D space in Figure 5-20 and Figure 5-21.
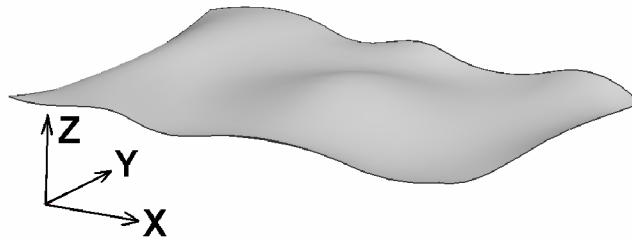
Figure 5-19: Example surface.
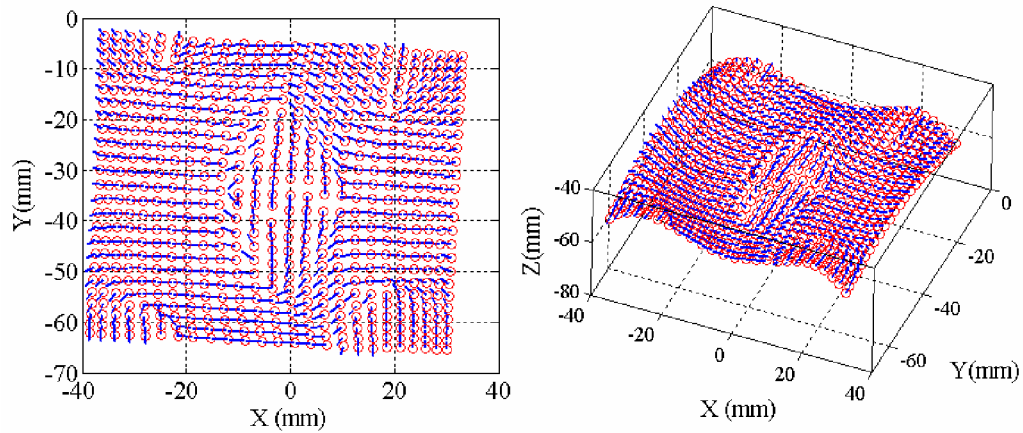
Figure 5-20: First principal curvature, κ_{n_1}.
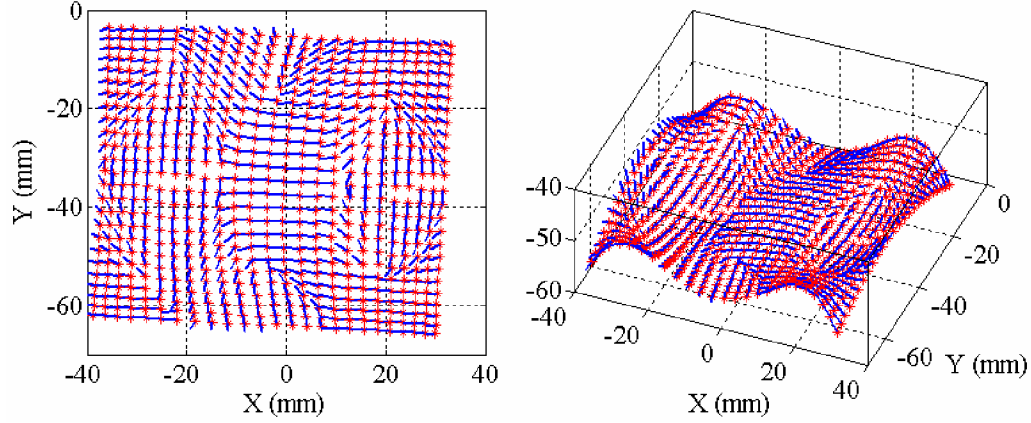
Figure 5-21: Second principal curvature, κ_{n_2}.

Maximum available tool radius for a given surface is determined with respect to the maximum and minimum principal curvatures of the surface. If the maximum normal curvature of the surface, κ_{n_1}, is positive, curvature of the cutter must be greater than κ_{n_1} in order to have a gouge-free machining at that cutter contact point. For ball-end mill cutters, curvature is given as follows:

$$\kappa_{Tool} = \frac{1}{R_{Tool}} \tag{5.17}$$

Therefore the following condition should hold

$$\kappa_{n,1} \leq \kappa_{Tool} \tag{5.18}$$

So, maximum available tool radius is determined as below.

$$R_{max} = \frac{1}{\kappa_{n,1}} \tag{5.19}$$

5.5   Clustering the Local Machining Directions

The vector field of the optimal cutting directions, F, needs to be partitioned into sub-regions on which a single machining pattern can be applied. In the literature, several clustering and partitioning algorithms are proposed. A clustering algorithm based on graph theory is efficient when applied on vector field clustering [6],[28]. In

this thesis, Normalized Cuts algorithm proposed by Shi, et al. [28] is applied for clustering purpose. The normalized cuts algorithm is a non-average technique. Therefore the resulting number of clusters does not depend on initial choice of number of clusters unlike other algorithms such as K-means. The normalized cuts algorithm solves an eigensystem in order to cluster given vector field.

The vector field F is considered as a weighted graph G, where nodes correspond to the vectors and the connections are constructed by every pair of nodes. Similarity between nodes "i" and "j" is defined as the weight value w_{ij}, where w_{ij} is the elements of the weight matrix, W. The aim is maximizing the similarity of nodes within a subset while minimizing the similarity of nodes across different sub-sets. The normalized cuts algorithm defines N_{cut} as criterion to partition the graph G, into groups G_1 and G_2, which is given as follows:

$$Ncut(G_1,G_2)=\frac{cut(G_1,G_2)}{assoc(G_1,G)}+\frac{cut(G_1,G_2)}{assoc(G_2,G)} \tag{5.20}$$

where, $cut(G_1,G_2)=\sum_{l\in G_1,k\in G_2} w_{lk}, assoc(G_1,G)=\sum_{l\in G_1,t\in G} w_{lt}$. Since N_{cut} is the criterion for measuring the goodness of a partition it is intended to minimize the value of N_{cut}. In order to do this, the initial graph G should be partitioned such that $cut(G_1,G_2)$ is minimized and $assoc(G_1,G)$ is maximized. This is performed by solving the following standard eigensystem.

$$\mathbf{C}^{-\frac{1}{2}}.(\mathbf{C}-\mathbf{W}).\mathbf{C}^{-\frac{1}{2}}z=\lambda z \tag{5.21}$$

where,

$$c_i=\sum_{j=1}^{N} w_{ij} \text{ and } \mathbf{C}=\begin{bmatrix} c_1 & 0 & ... & 0 \\ 0 & c_2 & ... & ... \\ ... & ... & ... & 0 \\ 0 & ... & 0 & c_N \end{bmatrix}.$$

Signs of the components of the second smallest eigenvector are used as the indicators to partition the vector field. Vectors associated with the same sign are assigned to the same sub-group. This procedure is repeated recursively until N_{cut} is below a pre-defined value. Although the partitioning is controlled by threshold value of

N_{cut}, in some cases it may be required to apply a refinement algorithm on the partitioned graph. The weight matrix, W is calculated as follows:

Let $\mathbf{f_i}=[f_{ix}\ f_{iy}\ f_{iz}]^T$ is located at $\mathbf{x_i}==[x_i\ y_i\ z_i]^T$

$$w_{ij}=\alpha.e^{-dist_{ij}}+(1-\alpha).e^{-diff_{ij}} \tag{5.22}$$

where,

$$0<\alpha<1,\ dist_{ij}=\sqrt{(x_i-x_j)^2+(y_i-y_j)^2+(z_i-z_j)^2}\ ,\ and\ diff_{ij}=\sqrt{(f_{ix}-f_{jx})^2+(f_{iy}-f_{jy})^2+(f_{iz}-f_{jz})^2}$$

Parameter α is used to adjust the emphasis on difference in vectors and vector locations.

5.6   Summary

In this section, the methodologies for evaluation and selection of machining strategies are presented. Since material removal rate is relatively high in roughing operations the tool is subjected to high cutting forces. Thus, while evaluating machining strategies process mechanics is taken into consideration. Several number of control points are selected on the surface. At each control point, several local machining directions are evaluated based on force simulations. The direction with the lowest penalty is chosen to be the local machining direction at that control point. On the other hand, material removal rate is relatively low and resulting surface quality is of great importance. Therefore, the intrinsic properties of the given surface are considered in machining strategy evaluation for finishing operations. The methodology used for roughing operations can be extended to finishing operations by relating the penalty function to tool deflection. Besides, the determined vector field of local machining directions is clustered using the normalized cuts algorithm.

Chapter 6

Applications

6.1   Introduction

In this chapter, application of the proposed methodologies on different cases is illustrated. Machining strategy evaluation for roughing is applied on 2 example geometries which are shown in Figure 6-2 and Figure 6-4. For each case force simulations are performed under the machining conditions given in Table 6-1 and Table 6-4 respectively. Two different radial depth of cut value are considered in the second example, where machining strategy for a complex surface is investigated. This is to examine the effect of radial depth of cut on machining strategy selection. Also, 3 machining strategies, Zig, Zig-Zag and Follow periphery are applied on both surfaces. The strategies are illustrated in Figure 6-1. The strategies are compared from process mechanics and machining time points of view. The proposed method for minimization of the total machining time is applied on roughing pass of a die shown in Figure 6-9.
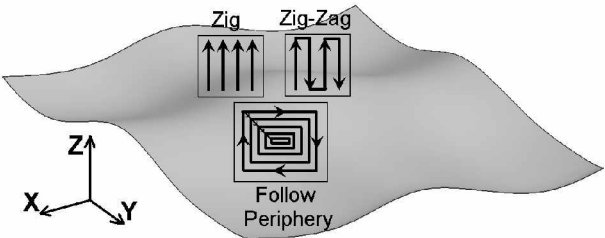
Figure 6-1: Applied strategies.

6.2 Machining Strategy Evaluation

6.2.1 Application 1: Airfoil Surface

In this application, the proposed methodology is applied on an airfoil surface shown in Figure 6-2. Machining conditions are given in Table 6-1.
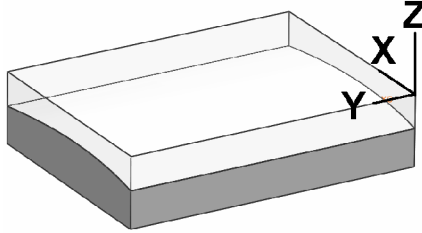
Figure 6-2: Airfoil surface.

Tool	6 mm (ball-end), 2 fluted
Tool Axis	Lead =5, Tilt=5 deg.
Grid Size	15 X 15
Radial depth of cut (% of tool diameter)	80
Milling mode	Down
W_D	0.5
# of steps for time calculation	20
# of points per step for time calculation	100

Table 6-1: Machining conditions for 1st application.

The selected local directions are shown in Figure 6-3. As it is seen, the proposed machining strategy has linear pattern and in "v" direction. The vector field of selected cutting directions does not require any clustering as it is seen. Thus, the clustering algorithm is not applied on the determined vector field.
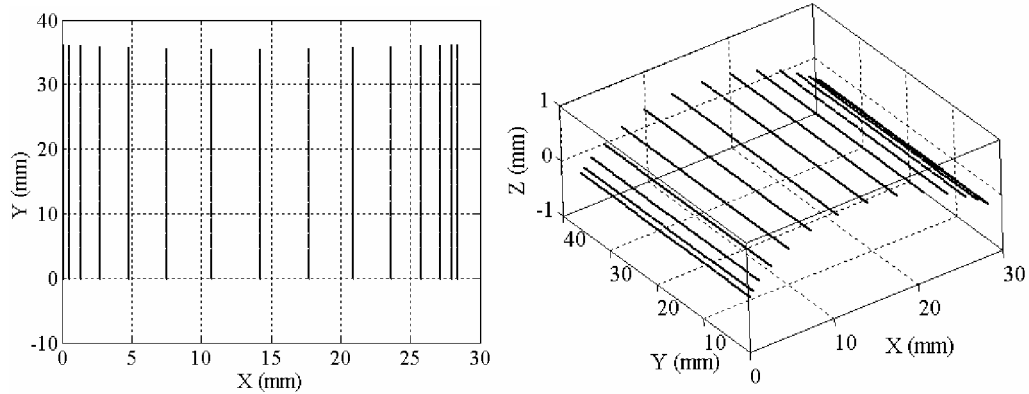
Figure 6-3: Selected local directions.

Three machining strategies are applied on the surface and the results are compared. Simulations are performed under the machining conditions given in Table 6-2. For zig and zig-zag patterns two different cases are considered, where the cutting directions are in "u" and "v". In other words, for zig and zig-zag strategies cutting steps are parallel to "x" axis in the first case and "y" axis in the second case. Also, the approximate machining time for each strategy is calculated. The comparison is given in Table 6-3.

Tool	6 mm (ball-end), 2 fluted
Tool Axis	Lead =5, Tilt=5 deg.
# of grid points	10 X 10
Radial depth of cut (% of tool diameter)	50

Table 6-2: Machining conditions in strategy comparison

	Zig		Zig-Zag		Follow Periphery
	"u"	"v"	"u"	"v"	
Machining Time	0.81		0.77		0.60
Total penalty Due to Force deviation	2183	0	2245	0	1304
Total penalty due to force magnitude	9744	9721	9750	9721	9600
Total Penalty	11927	9721	11995	9721	10905
Average Penalty	119.27	97.21	119.95	97.21	109.05

Table 6-3: Strategy comparison

As it is seen in Table 6-3 even the machining strategy is known, the cutting direction is also important from process mechanics point of view. Force penalty values are smaller when cutting direction is in "v". It should be noticed that results of strategy comparison and strategy determination shows agreement in cutting direction and strategy pattern. It is also seen that, the minimum machining time is obtained by follow periphery pattern.

6.2.2 Application 2: Complex Surface

In this application, the proposed methodology is applied on a complex surface shown in Figure 6-4. Machining conditions are given in Table 6-4. In this case, two different radial depth of cuts values are used in order to investigate the effect of radial depth of cut on selection of local machining directions.
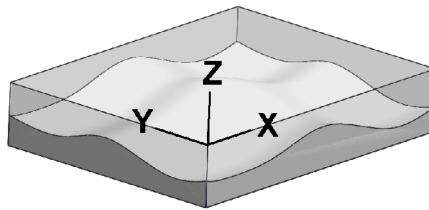
Figure 6-4: Complex surface

Tool	12 mm (ball-end), 2 fluted
Tool Axis	Lead =5, Tilt=5 deg.
# of grid points	15 X 15
Radial depth of cut (% of tool diameter)	50 and 80
Milling mode	Down
W_D	0.5
# of steps for time calculation	20
# of points per step for time calculation	100

Table 6-4: Machining conditions for 2nd application

The selected local directions are plotted in Figure 6-3 and Figure 6-7 for 50% and 80% radial depth of cut values respectively. As it is seen, it is required to apply

clustering on the vector field. The clusters after a first level clustering is plotted in Figure 6-6 and Figure 6-8 for 50 % and 80 % radial depth of cut values respectively.
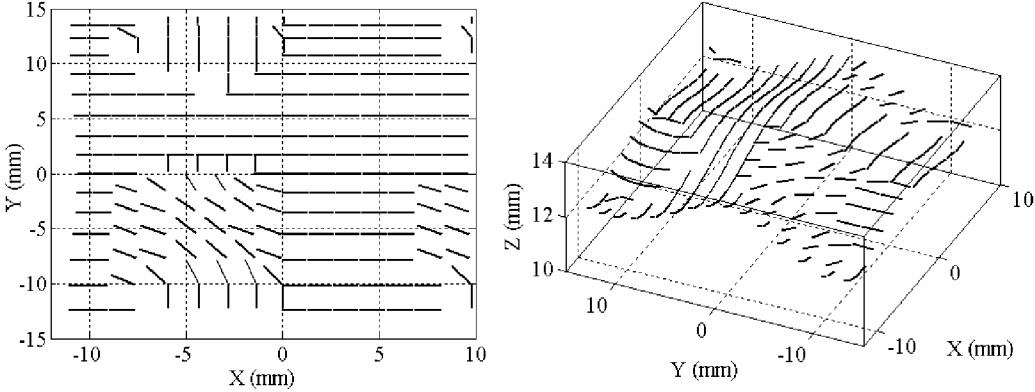
Figure 6-5: Selected local directions. (Radial = 50 %)
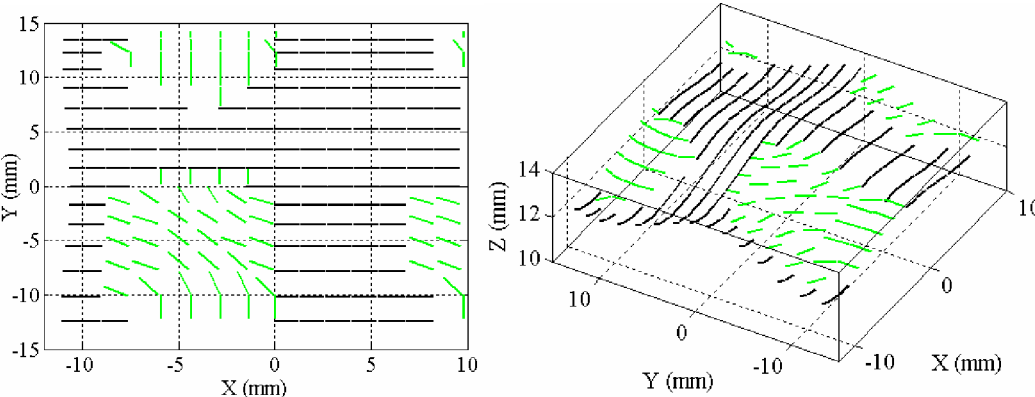
Figure 6-6: Clustered local directions. (Radial = 50 %)
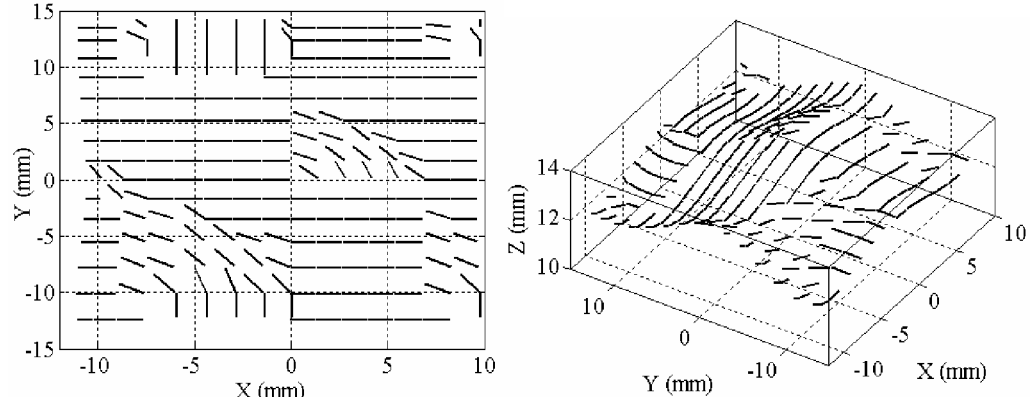
Figure 6-7: Selected local directions. (Radial = 80 %)
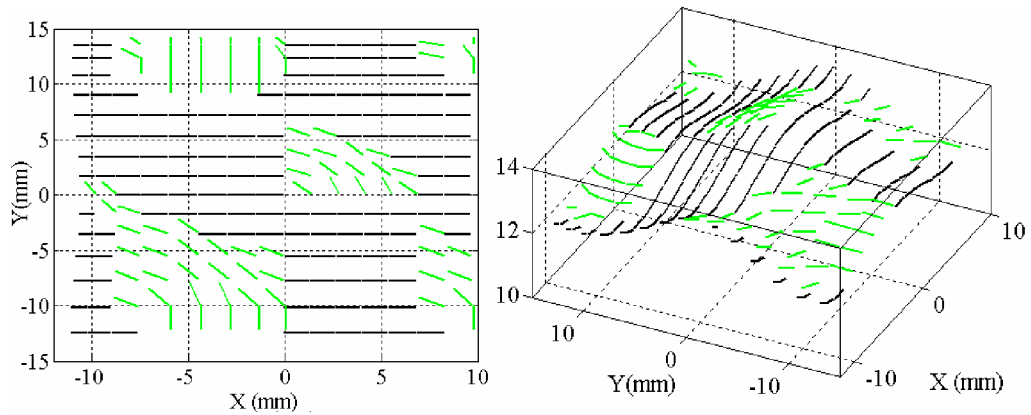
Figure 6-8: Clustered local directions. (Radial = 50 %)

When the determined directions for each radial depth of cut value are examined it is seen that radial depth of cut affects the selection of optimal local cutting direction. Therefore, it can be concluded that, before performing a strategy evaluation, radial depth of cut value should be known beforehand.

	Zig		Zig-Zag		Follow Periphery
	"u"	"v"	"u"	"v"	
Machining Time (min)	0.48		0.44		0.33
Total penalty Due to Force deviation (N)	2082	3421	1732	3452	2665
Total penalty due to force magnitude (N)	8916	8452	9012	8634	8413
Total Penalty (N)	10988	11874	10744	12086	11078
Average Penalty (N)	109.88	118.74	107.44	120.86	110.78

Table 6-5: Strategy comparison

In Table 6-5 it is again seen that, the cutting direction is important from process mechanics point of view. Force penalty values are smaller when cutting direction is in "u" in this application. It should be noticed that results of strategy comparison and strategy determination shows agreement in cutting direction. It is also seen that, the minimum machining time is obtained by follow periphery pattern.

6.3   Total Machining Time Minimization

6.3.1   Optimization of Roughing Process

The die geometry shown in Figure 6-9 is selected as the workpiece which is scaled to 1/4 of its original size. Tool path is generated for the blower section of the die with 1 mm of axial depth of cut increments and 0.1 mm radial depth of cut. Tool path is illustrated in Figure 6-10. The geometry has a maximum depth of 22 mm. Thus, there are 22 axial layers in the tool path. Stable depth of cut pairs for axial depths 1, 2…, 5 mm are obtained. Pairs of stable limits of axial and radial depths of cut and feasible feed per tooth for spindle speed around 9000 rpm are presented in Table 6-8. Since slotting causes accelerated tool wear, b_{lim} values greater than 0.8 are chosen as 0.8. Larger axial depth of cut values could be used; however the force model is applicable to cases where the ball-end mill of the cutter is in contact with the workpiece. Thus, only the axial depth of cut values smaller or equal to tool radius are taken into consideration. However, the force model can also be extended to the cases where the cylinder part of the tool is in cut which is currently an on going research in our laboratory.
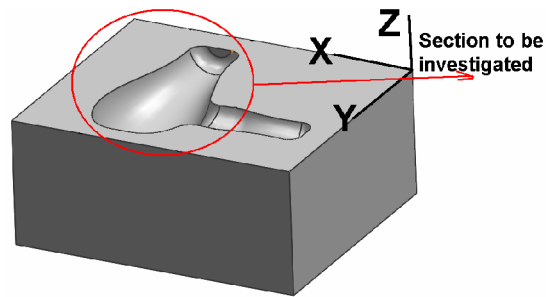
Figure 6-9: Workpiece geometry.
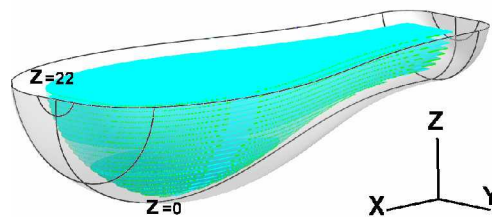
Figure 6-10: The generated tool path.

65

In stability analysis, the milling system with the dynamic properties given in Table 6-6 is taken into consideration [33].

ω_{nx}	600 Hz
ω_{ny}	660 Hz
k_x	5600 kN /m
k_y	5600 kN /m
ζ_x	0.035
ζ_y	0.035
K_t	600MPa
K_r	0.07
Milling mode	Up milling
# of flutes	2

Table 6-6: Parameters for the milling system used in stability analysis.

For 2 mm of axial depth of cut variation of stable radial depth of cut with the spindle speed is given in Figure 6-11.
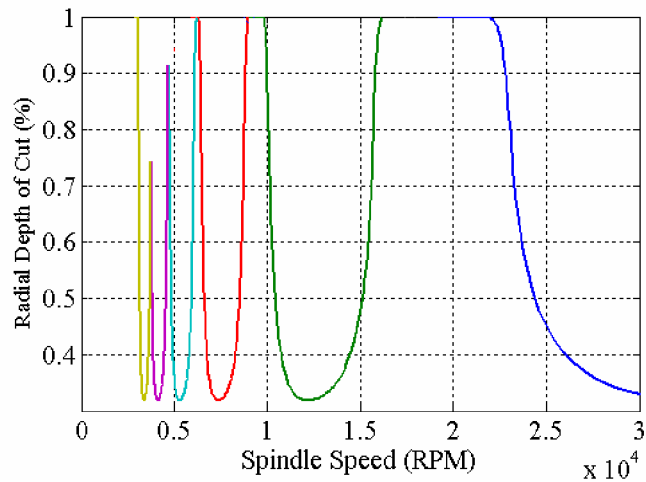
Figure 6-11: Spindle speed vs. radial depth of cut diagram (a=2 mm)

Available feed per tooth range, cutter geometry, and mechanical properties of the machine tool are given in Table 6-7.

Max fpt	0.1
Min fpt	0.02
Tool diameter	10 mm
Spindle Torque (~9000 rpm)	15 Nm
Spindle Power (~9000 rpm)	20 W
Tool Life (~9000 rpm)	50 min.

Table 6-7: System parameters.

Axial Depth (mm)	b_lim	Feasible fpt (mm/rev)
1	1	0.1
2	1	0.1
3	1	0.1
4	0.83	0.1
5	0.57	0.1

Table 6-8: Pairs of stable limits of axial and radial depths of cut (around 9000 RPM)

The optimized values are compared with a conventional case in Table 6-9. The conventional case presents the values chosen without any insight in process dynamics and mechanics. Therefore, the chosen values are conservative. On the other hand, once the process dynamics and mechanics are taken into consideration, those conservative parameters can be improved.

	Conventional	Optimized
Axial Depth	2	4
Radial Dept	60 %	80%
Feed (mm/tooth/rev)	0.05	0.1
Machining Time	2 min	0.72 min

Table 6-9: Comparison of optimized and conventional cases

6.4   Correcting Actual Feed Rate Problem in Simultaneous 5-Axis Milling

In Computer Aided Manufacturing (CAM) software environment, always the tool is in motion and the workpiece is stationary. However, in real simultaneous 5-axis milling operations, the workpiece may have absolute motion depending on the configuration of the machine tool. In such cases the resultant relative velocity, i.e. the cutting feed rate, is a result of the absolute movements of the individual axis. Although these two are equivalent for 3 axis applications involving linear motions only, in case of 5-axis motions significant differences may result yielding incorrect feed rates depending on the way the CNC interprets the 5-axis feed rate commands. In general, the feedrate can be defined by the "F" command in three modes which are mm/min (G94), rev/min (G93), and mm/rev (G95). The first two of those are used when the machining axes are

translational and the last one is used when rotational respectively. In most of the cases, machining axes are translational ones. If feed rate is provided in G94 mode, the programmed feed rate value does not apply for the synchronized rotational axes [29]. In G94 mode, feed rate is defined once and it is kept constant until the motion is completed. Since the defined feed rate does not apply for the synchronized rotational axes, the relative cutting feed between the tool and workpiece decreases. On the other hand, in G93 mode, instead of feed rate, the inverse of time required to complete each line of the part program is defined. For example, "F2" means that the completion time for that line is ½ minutes. Thus, the relative cutting velocity is kept constant. In order to solve such a problem, the CL file is used and the following steps are applied.

i.   The CL file is parsed.
ii. The distance between each tool position is calculated
iii. Time required to complete each program line is calculated by diving the distance to linear feed rate which is defined beforehand
iv. The inverse of the time is calculated as inverse time feed rate.

Chapter 7

Conclusions and Future Work

5-axis milling is widely used in high precision complex surface machining industries. It provides high motion capability and increased cutter accessibility, which complicates the geometry and mechanics of 5-axis milling processes. The geometry of 5-axis milling operations is modeled and an existing process model is integrated with the geometrical analysis methods in order to perform cutting force simulation along a given toolpath. In addition, optimization models are developed in order to optimize those processes.

There are several constraints which have to be considered in optimization of 5-axis milling operations. Those can be named as, cutting force, cutting torque, cutting power, chatter vibrations, tool & part deflections and maximum chip thickness. Cutting torque and power are limited to the available cutting torque and power on the spindle. Also, the process should be chatter-free. In order to keep dimensional quality above a certain level tool deflections must be limited.

In this study, as the first step process geometry is analyzed. CL-file is used as the main information source. Position and orientation of the tool is parsed using the developed CL-file parser module. Then, those are used together with the analytical information of workpiece geometry in order to extract geometrical parameters such as depth of cuts, lead and tilt angles. The proposed geometrical analysis methods are applied on two complex surfaces for verification purpose. It is observed that, the desired parameters are calculated accurately. In addition, the geometrical model is integrated with the process model and cutting force simulation is performed along a toolpath which is generated for a bumped surface. The simulation is verified by cutting experiments. A good agreement is observed between the simulated and measured cutting forces. However some amount of discrepancy is observed in cutting force in Z

direction. This is due to the indentation forces created at the tool tip where the cutting edge can not cut to due to the fact that the cutting speed reduces to zero at the center. However, these forces can also be identified and included in the ball end milling model which is currently an on going research in our laboratory.

A process optimization model is developed to optimize tool orientation, machining parameters and machining strategy. This study is recognized as a first attempt to optimize 5-axis milling processes considering various limitations. In optimization of the tool orientation, variation of the resultant transversal cutting force, F_{xy}, is simulated among several combinations of lead and tilt angles under various radial depth of cut values. The simulations are verified by experimental results. It is observed that, as the radial immersion increases optimal value of tilt angle changes, where optimal value of lead angle does not change significantly. Machining parameters, such as feed rate, axial and radial depth of cuts are compromised to minimize the total machining time of roughing operations. Limitations such as chatter vibrations, tool life, spindle power, spindle torque and available feed per tooth are considered while minimizing the total machining time. In machining strategy optimization, roughing operations and finishing operations are considered separately since the requirements for each type of operation are different. In optimization of machining strategy in roughing operations, several grid points are formed on the surface. The required geometrical parameters are calculated along various cutting directions at each control point using the developed geometrical model in the first step of the thesis. Then, the cutting forces are simulated. With respect to the simulation results, penalty functions are calculated by assigning weight factors to force deviation and force magnitude along each direction. For finishing operations, the intrinsic properties of the given surface are examined. The developed method for roughing operations can be applied on finishing operations, by re-defining the penalty function as tool deflection. In addition, a model in order to calculate the machining time for a given surface and machining conditions is proposed.

Finally, the proposed methods are applied on various workpiece geometries and results are presented. It is shown that, cutting direction and machining strategy patterns is of great importance from process mechanics point of view. Machining time of each strategy is calculated and presented. As a real world problem in 5-axis simultaneous milling, actual cutting feed rate problem is solved by using the CL file parser module.

As a future work, the geometrical model can be integrated with a geometrical engine in order to add visualization to the geometrical analysis. This may be beneficial

to extend the geometrical model to more complex cases where holes, key ways, sharp corners etc. exist on the workpiece surface. The process simulation technique can easily be integrated with a commercial CAD/CAM system in order to add extra capabilities to current CAD/CAM systems. In addition, the model developed for process optimization can be extended in order to perform a larger scale optimization for 5-axis milling operations.

In this thesis, a geometrical model for 5-axis milling operations is developed for process simulation and optimization purposes considering various limitations. This is not present in the literature. It is seen that by using the methodologies proposed in this thesis the productivity and part quality can be improved. This thesis forms a basis for the forthcoming studies in simulation and optimization of 5-axis milling processes.

Bibliography

[1] Anderson, R. O., Detecting and eliminating collisions In NC Machining, Computer-Aided Design, Vol.10 No.4, 231-237,1978.

[2] Bailey, T. Elbestawi, M.A., El-Wardany, T.I., Fitzpatrick, P., Generic simulation approach for multi-axis machining, Part 1: Modeling methodology, Transactions of ASME, 124, 624, 2002.

[3] Bailey, T. Elbestawi, M.A., El-Wardany, T.I., Fitzpatrick, P., Generic simulation approach for multi-axis machining, Part 2: Model calibration and feed rate scheduling, Journal of Materials Processing Technology, 103, 398-403, 2000.

[4] Baptista, R., Simoes, J.F.A., Three and five axis milling of sculptured surfaces, Journal of Materials Processing Technology, 103,398-403, 2000.

[5] Chappel, I.T, 1983, The use of vectors to simulate material removed by numerically controlled milling, Computer-Aided Design, 15(3), May, 156-8.

[6] Chen, J.L. Bai, Z. Hamman, B. Terry, J.L., A Normalized-cut algorithm for hierarchical vector field data segmentation.

[7] Choi,B.K., Surface modelling for CAD/CAM, Elsevier, New York 1991.

[8] Choi,B.K. ,Jerard, R.B., Scultptured surface machining, theory and applications, 04127820208, Kluwer Academic Publishers, Dordrecht, 1998.

[9] Chu, Bohez, A.M. Makhanov, E.L.J. Munlin, S.S. Phien, M. H.N. Tabucano, M.T., On 5-Axis freeform surface machining optimization: Vector clustering approach, Int. Journal of CAD/CAM.

[10] Du. S, Surmann,T., Webber, O., Weinert, K., Formulating swept profiles for Five-Axis tool motions, International Journal of Machine Tools & Manufacture, 45, 849-861, 2005.

[11] Erdim, H. Lazoglu, I. Ozturk, B., Feedrate scheduling strategies for free-form surfaces, International Journal of Machine Tools And Manufacture, Volume 46, Issues 7-8, 747-757.

[12] Fussel, B.K., Jerard, R.B., Hemmett, J.G., Modeling of cutting geometry and forces for 5-Axis Sculptured Surface machining, Computer Aided Design, Vol. 35, 333-346, 2003.

[13] Giri, V. Bezbaruah, D. Bubna, P. Choudhury, A.R., Selection of master cutter paths in sculptured surface machining by employing curvature principle, Int. Journal of Machine Tools & Manufacture, 45, 1202-1209, 2005.

[14] Imania, B.M. Sadeghib, M.H., Elbestawia, M.A., An improved process simulation system for ball-end milling of sculptured surfaces, International Journal of Machine Tools & Manufacture, 38 , 1089-1107, 1998.

[15] Kim, G.M. Cho, P.J. Chu, C.N. Cutting force prediction of sculptured surface ball-end milling using Z-Map, Mach. Tool & Manufacturing, 40, 277–291, 2000.

[16] Kim, Y.H. Ko, S.L., Development of searching algorithm to predict cutting regions using octree method, 3rd International Conference And Exhibition On Design And Production of Dies And Molds, June 17-19, 2004, Bursa, Turkey, DM 2004-46, Pp.59-65

[17] Lacalle, L.N.L Lamikiz, A. Sanchez, J.A. Saldago, M.A., Toolpath selection based on the minimum deflection cutting forces in the programming of complex surfaces milling, Int. Journal of Machine Tools & Manufacture, Article In Press.

[18] Lazoglu, I., Sculptural surface machining: A generalized model of ball end milling force system, International Journal of Machine Tool & Manufacturing, 43, 453-462,2003.

[19] Lee, T. S., Lin Y. J., A 3D predictive cutting-force model for end milling of parts having sculptured surfaces, Int J Adv Manufactuing Technology, 16, 773-783, 2000.

[20] Lee, S.K. Ko, S.L, Development of simulation system for machining process using enhanced Z Map model, Journal of Materials Processing Technology, Volumes 130-131, 20, 608-617,2002.

[21] Lim, EE. M., Menq, C.H., Integrated planning for precision machining of complex surfaces. Part 1: cutting-path and feedrate optimization, Int. J. Mach Tools Manufact., 37-1, 61-75, 1997.

[22] Lim, T.S. Lee, C.M. Kim, S.W. Lee, D.W., Evaluation of cutter orientations In 5-Axis high speed milling of turbine blade, Journal of Materials Processing Technology,130,401-406, 2002.

[23] Meng, EE.L., Feng,H.Y., Menq, C.H., Lin, Z.H., The prediction of dimensional errors for sculptured surface productions using the ball-end milling process Part 1: Chip geometry analysis and cutting force prediction, International Journal of Machine Tools & Manufacture, 35-8, 1149-1169, 1995.

[24] Ming, C.H., Hwang, Y.R., Hu, C.H., Five-Axis tool orientation smoothing using quaternion interpolation algorithm, International Journal of Machine Tools & Manufacture , 43,1259-1267, 2003.

[25] Ozturk, B., Lazoglu, I., Machining of free-form surfaces. Part I: Analytical chip load, International Journal of Machine Tools And Manufacture, Volume 46, 7-8, 728-735, 2006.

[26] Ozturk, E., Budak,E., Modelling of 5-Axis milling forces, 8th CIRP International workshop on modeling of Machining Operations, Chemnitz, Germany, 319-326, ,2005.

[27] Ramos, A.M., Relvas,C., Simoes, J.A., The influence of finishing milling strategies on texture, roughness and dimensional deviations on the machining of complex surfaces, Journal of Materials Processing Technology, 136, 209-216, 2003.

[28] Shi, J. Malik, J., Normalized cuts and image segmentation, IEEE Transactions On Pattern Analysis And Machine Intelligence, 22, 888-905, 2000.

[29] Siemens, SINUMERIK 840D/840Di/810D/FM-NC Fundamentals.

[30] Tekeli, A. Budak, E., Maximization of chatter-free material removal rate in end milling using analytical methods, Machining Science And Technology, 9, 147-167, 2005.

[31] Voeckel, H.B, Hunt, W A., The Role of Solid Modeling In Machining-Process Modeling And NC Verification, SAE Technical Paper 810195.

[32] Walstra W.H., Bronsvoort W.F.,Vergeest J.S.M, Interactive Simulation of Robot Milling For Rapid Shape Prototyping, Computer & Graphics, Vol.18 No.6, 861-871,1994.

[33] Weck, M., Altintas, Y., Beer, C., CAD Assisted Chatter Free NC Tool Milling. International Journal of Machine Tools and Manufacture, 34:879–891, 1994.

[34] http://www.spatial.com/components/acis

[35] http://mathworld.wolfram.com/Line-PlaneIntersection.html

[36] http://www.ugs.com/products/nx/